NASA Technical Paper 3613

Comparison of Extravehicular Mobility Unit (EMU) Suited and Unsuited Isolated Joint Strength Measurements

David A. Morgan
Robert P. Wilmington
Abhilash K. Pandya
James C. Maida
Kenneth J. Demel

June 1996

NASA Technical Paper 3613

Comparison of Extravehicular Mobility Unit (EMU) Suited and Unsuited Isolated Joint Strength Measurements

David A. Morgan, Robert P. Wilmington, and Abhilash K. Pandya
Lockheed Martin Engineering & Sciences
Houston, Texas

James C. Maida and Kenneth J. Demel
Lyndon B. Johnson Space Center
Houston, Texas

June 1996

This publication is available from the NASA Center for Aerospace Information, 800 Elkridge Landing Road, Linthicum Heights, MD 21090-2934, (301) 621-0390

Abstract

In this study the strength of subjects suited in extravehicular mobility units (EMUs) – or Space Shuttle suits – was compared to the strength of unsuited subjects. The authors devised a systematic and complete data set that characterizes isolated joint torques for all major joints of EMU-suited subjects. Six joint motions were included in the data set. The joint conditions of six subjects were compared to increase our understanding of the strength capabilities of suited subjects. Data were gathered on suited and unsuited subjects. Suited subjects wore Class 3 or Class 1 suits, with and without thermal micrometeoroid garments (TMGs). Suited and unsuited conditions for each joint motion were compared. From this the authors found, for example, that shoulder abduction suited conditions differ from each other and from the unsuited condition. A second-order polynomial regression model was also provided. This model, which allows the prediction of suited strength when given unsuited strength information, relates the torques of unsuited conditions to the torques of all suited conditions. Data obtained will enable computer modeling of EMU strength, conversion from unsuited to suited data, and isolated joint strength comparisons between suited and unsuited conditions at any measured angle. From these data mission planners and human factors engineers may gain a better understanding of crew posture, and mobility and strength capabilities. This study also may help suit designers optimize suit strength, and provide a foundation for EMU strength modeling systems.

Acknowledgments

This research was supported by NASA contract no. NAS9-18800. The authors wish to thank members of the Graphics Research and Analysis Facility and the Anthropometry and Biomechanics Laboratory at the Lyndon B. Johnson Space Center (JSC) for assistance in developing and reviewing this report. The authors also wish to thank the Crew and Thermal Systems Division (JSC) for supplying the space suits and for assisting with protocol development and restraint mechanisms. Special thanks are extended to Mr. Glenn Klute for assisting in the initiation of this study, and to Ray McKenna for his elaborate review of this project. We also acknowledge the significant contributions of Ralph Wemhoff, Barbara Woolford, and Lorraine Hancock.

Contents

Tables

Figures

Acronyms

ab/ad	abduction/adduction
ABL	Anthropometry and Biomechanics Laboratory
CTSD	Crew and Thermal Systems Division
EMU	extravehicular mobility unit
EVA	extravehicular activity
f/e	flexion and extension
GRAF	Graphics Research and Analysis Facility
JSC	Lyndon B. Johnson Space Center
N/A	not applicable
PC	portable computer
PLSS	portable life support system
psid	pounds per square inch differential
ROM	range of motion
rot	rotation
TMG	thermal micrometeoroid garment
WETF	Weightless Environment Training Facility

Suit Abbreviations and Definitions:

ux	unsuited
1u	Class 1 suit, no TMG
1t	Class 1 suit with TMG
3u	Class 3 suit, no TMG
3t	Class 3 suit with TMG
Ave	average of all four suited conditions

1. Introduction

Strength limitations of the extravehicular mobility unit (EMU) – the Space Shuttle suit – are not well understood. Severe strength and research limitations are imposed by the EMU suit. No comprehensive strength data exist for the isolated joints of an EMU-suited crew member as compared with that crew member's unsuited strength. In this study, isolated joint strength data in both the suited and unsuited condition were collected and processed. The Flight Crew Support Division's Anthropometry and Biomechanics Laboratory (ABL) and the Graphics Research and Analysis Facility (GRAF), in cooperation with the Crew and Thermal Systems Division (CTSD), have completed a study in which quantitative data for the isolated joint strength capability of six suited operators were collected and processed. A generic methodology has also been established that quantifies the differences between and within the unsuited and different suited conditions.

Overall the goal of this study was to extend the current EMU strength database. This was achieved by systematically and comprehensively assessing the strength of the major joints of an EMU-suited subject, and by comparing the subject's suited strength with that subject's unsuited strength. Five conditions were compared. The subject was:

- suited in a Class 1 suit, which is acceptable for flight use, with a thermal micrometeoroid garment (TMG)
- suited in a Class 1 suit, without a TMG
- suited in a Class 3 suit, which is acceptable for non-hazardous training or display purposes, with a TMG
- suited in a Class 3 suit, without a TMG
- unsuited

Six joint motions were included in the study. They are: (1) elbow flexion and extension, (2) wrist flexion and extension, (3) shoulder flexion and extension, (4) shoulder abduction and adduction, (5) shoulder internal and external rotation, and (6) knee flexion and extension. Because of this information, the NASA community is provided with a computer-ready database of EMU strength data. The report also provides a prediction capability (within the scope of data collection) of the EMU-suited strength of an individual when given that individual's easily measured unsuited strength profile.

Information in this report could assist mission planners and human factors engineers in understanding crew strength capabilities. Moreover, the data gathered could allow them to design and distribute physically demanding task assignments that would take full advantage of a suited crew member's capabilities. Extravehicular activity (EVA) plans could also aid suit designers who might wish to optimize strength in future space suit designs. Finally, the strength data provided could form the basis of future EMU strength modeling systems (Fig. 1).

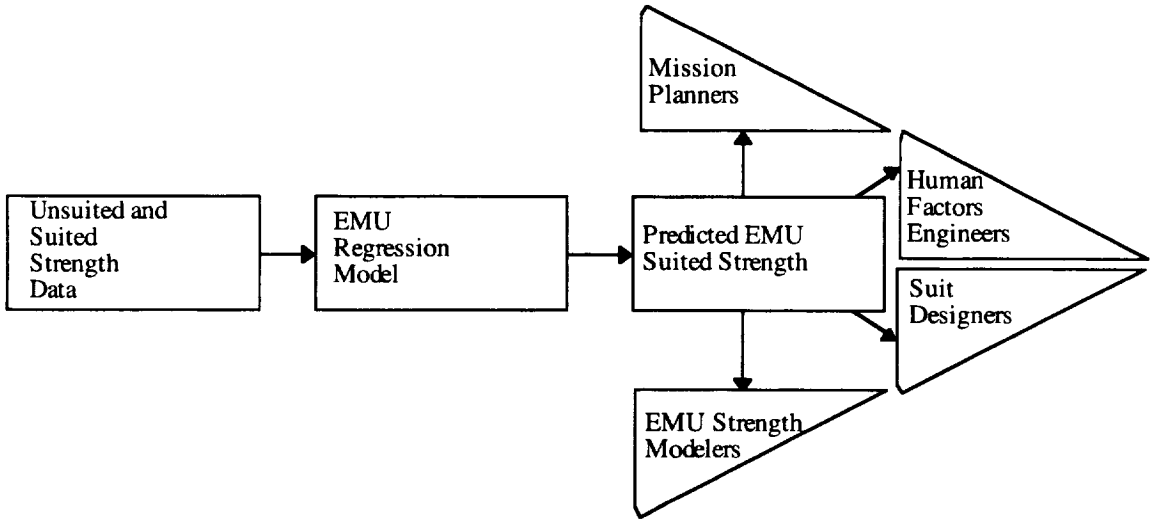

Figure 1 Utilization of EMU strength data

2. Methodology

2.1 The Extravehicular Mobility Unit

The design of the Shuttle EMU maximizes the mobility of suited crew members and minimizes the fatigue experienced on EVAs. The EMU is a constant volume, constant pressure (4.3 ± 0.1 psid) system. It uses several different techniques to assist in maximizing an EMU operator's mobility. Suit mobility is primarily increased through introducing bearings at key locations throughout the space suit. For example, the space suit arms have three bearings. These are the: (1) scye bearing at the shoulder, (2) arm bearing proximal to the elbow, and (3) glove bearing proximal to the wrist. Another feature that enhances mobility is the convoluted material on the outside of the elbow and knee joints. This material allows the joints to be moved through their range of motions while still keeping them at an approximately constant volumes. Relatively constant volumes are maintained because, as the joints are operated, convolutes are being collapsed while other convolutes are being opened. This series of convolutes not only helps to maintain relatively constant volumes, it also acts as a cloth-hinge joint. Suit pressurization causes the suit's knee and elbow joints to revert towards a single joint angle. This position, which is slightly less than the fully extended position of each joint, is based on the neutral body posture presented in NASA STD-3000. Thus, when a subject performs knee flexion and extension, some resistance to flexion of the knee could be expected, especially in extreme cases, and some assistance in extension of the knee from the flexed position could also be expected. This occurs because of pressurization up to the neutral body posture, at which point the suit design would require increased effort for further extension.

2.2 Apparatus

Strength measurements were performed on a LIDO Multi-Joint II testing unit (Fig. 2) (Loredam Biomedical, Inc., West Sacramento, Calif.). The LIDO Multi-Joint II is an integrated system which consists of an isokinetic dynamometer connected to a portable computer (PC). The system comes with a series of attachments, which supports the strength measurements of various joints of the human body, and a bench, which allows for proper restraint and isolation of those joints. Software provides the operator with precise control of the actuator head during various modes of operation (isometric, concentric, eccentric, etc.). The system follows experiment-defined exercise parameters (range of motion (ROM), torque limits, velocity, number of repetitions, etc.). A unique feature of the system is that it outputs data in a machine-readable format for more customized data analyses. Also, the system incorporates a gravity compensation feature that takes into account the weight of hardware and the limb throughout the range of motion. This capability was used to remote the effect of the weight of the suit, the apparatus, and the test subject's limbs in the one-gravity (Earth) testing environment. From this, strengths that would be observed in a weightless environment were ascertained.

The LIDO Multi-Joint II has an adjustable workbench. This workbench can be easily manipulated to support either seated or reclined unsuited subjects for a wide variety of strength measurements. Measurements taken in this study required both unsuited and EMU-suited operators. Standard Shuttle EMU suits of types Class 1 (those acceptable for flight use) and Class 3 (those acceptable for non-hazardous training or for display purposes), which are equipped for external air supplies, were used for our investigation. As another set of conditions, the suit was outfitted with the TMG. An environmental control system maintained the suit pressurization level at 4.3 psid. During testing, an overhead crane relieved the test subject of the weight of the suit (which was approximately 260 to 270 lbs).

Because the portable life support system (PLSS) is positioned on the back of the Shuttle suit, no measurements could be taken of suited operators in a reclined posture. (A reclined posture is recommended by LIDO protocol.) To accommodate the use of the EMU for strength testing, additional hardware was developed. These modifications allowed the joint axis to be visually aligned with the LIDO actuator shaft. In addition, lab-specific support hardware was developed for the LIDO Multi-Joint II to accommodate the PLSS of the Shuttle suit for several suited isolated joint strength measurements. Support hardware consisted primarily of developing a second chair (Fig. 3). This chair and other hardware modifications to the restraint system were used to obtain isolated torque data for shoulder and elbow joints. The chair's construction simulated the LIDO bench configuration in a seated position. Its height was appropriate to accommodate a suited operator. The same backrest was used for both the LIDO bench and the newly constructed chair. Waist and wrist restraint straps were lengthened to accommodate the larger diameter of the suit. Additionally, modifications to the bracket on the elbow cuff created a thicker cross section so the cuff bracket would not bend with the extra weight of the EMU. Figures 4 and 5 are diagrams of the additional standard LIDO hardware attachments that were used to optimally isolate joints.

2.3 Subjects

Six male subjects took part in this experiment. All were right-handed. Their ages ranged from 28 to 55 years old, a range which represents the age range of the male crew population. All subjects who participated in this evaluation were required to have the current Air Force Class 3 physical prior to the experiment and to have a working knowledge of the use of a Shuttle space suit. Of the subjects who participated in this evaluation, all were given a full description of the testing procedures. All were asked whether they had any physical conditions that might keep them from participating in the experiment. Also, the subjects were given an informed consent form that described their right to withdraw from the experiment at any time, and possible side effects of maximal strength testing.

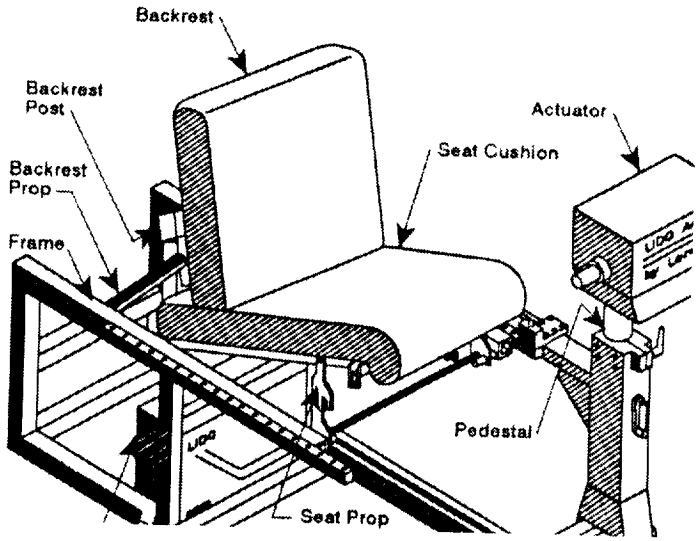

Figure 2 LIDO Multi-Joint II isokinetic dynamometer bench

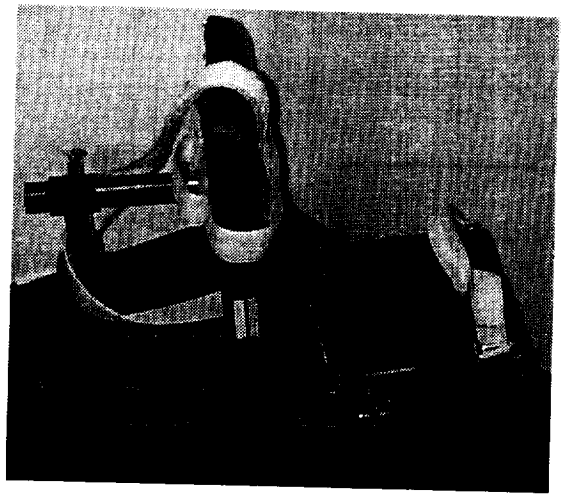

Figure 3 Additional hardware: restraints and external chair

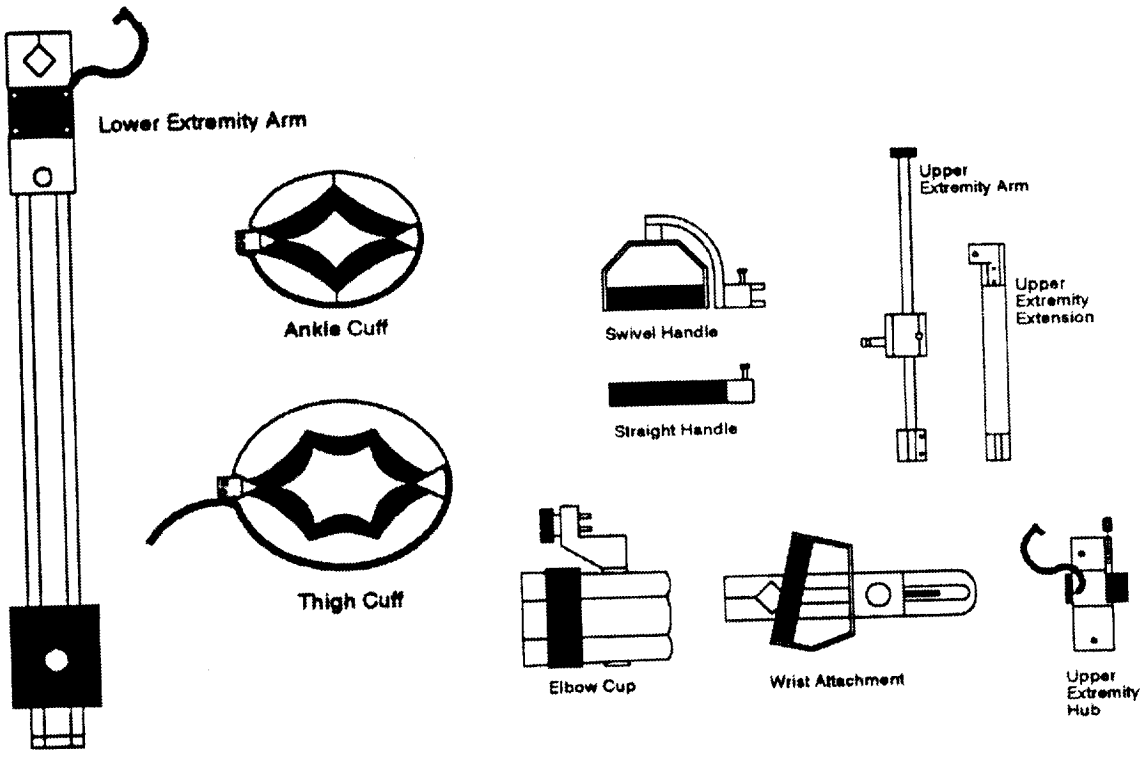

Figure 4 LIDO Multi-Joint II lower and upper extremity attachments
(reprinted from the LIDO manual)

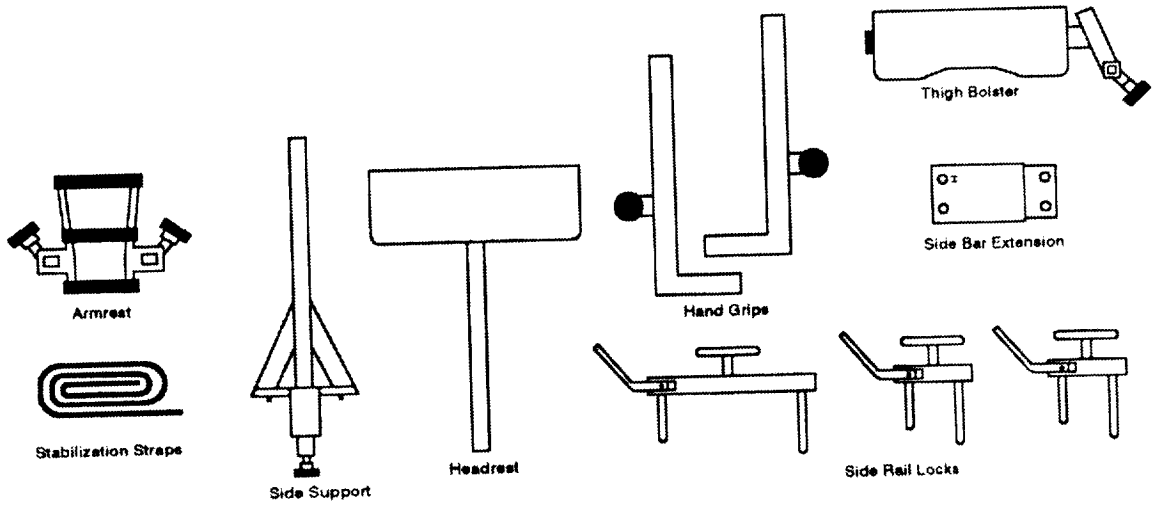

Figure 5. LIDO Multi-Joint II support attachments
(reprinted from the LIDO manual)

This test used a limited and expensive Class 1 suit, so only one size was available. Subjects were chosen based on size and on having similar anthropometric measurements. Table 1 summarizes the basic anthropometric measurements of the six subjects.

Table 1 Summary of Subjects' Anthropometric Measurements (in., lbs)

Anthropometric Measurements	*Subject 1*	*Subject 2*	*Subject 3*	*Subject 4*	*Subject 5*	*Subject 6*
Stature	68.0	67.8	68	69.5	69.2	68.1
Weight	170	139	160	135	160	155
Chest Breadth	12.7	12.75	12.3	12.6	12.3	14.0
Bi-Deltoid Breadth	18.5	17.7	16.9	17.8	17.8	18.5
Chest Circumference	38.0	35.4	39.0	37.0	40.1	37.0
Shoulder Circumference	45.8	40.1	43.5	43.7	46.0	43.3
Expanded Chest Depth	9.6	8.8	9.6	9.3	9.6	9.6
Head Length	7.8	7.7	7.8	8.0	7.7	8.2
Head Breadth	6.2	6.2	6.1	6.1	6.0	5.9
Vertical Trunk Diameter: R	24.8	25.0	26	24.8	26.3	26.9
Vertical Trunk Diameter: L	25.1	25.2	26.3	25.6	26.8	26.8
Hip Breadth	13.8	13.3	13.7	12.4	13.3	11.8
Tibia Height	19.4	18.8	18.1	20.4	19.0	20.5
Crotch Height	31.2	31.8	30.8	32.8	31.8	31.8
Mid Shoulder Height: R	55.5	56.7	56.3	57.2	58.0	57.5
Mid Shoulder Height: L	56.1	56.8	56.4	57.8	58.4	57.8
Shoe Size	8.5	8.5	10	10.5	9.5	7.5
Vertical Trunk Circumference: R	65.5	63.1	68.0	N/A	66.4	64.0
Vertical Trunk Circumference: L	66.8	63.0	68.5	N/A	66.5	65.0
Inter-Wrist Distance	53.8	55.1	N/A	55.8	57.4	54.5
Inter-Elbow Distance	32.8	35.4	N/A	36.2	37.4	35.3
Inter-Finger Tip Distance	67.6	69.4	66.9	70.4	72.0	68.3
Lower Arm Length: R	17.6	18.2	17.8	N/A	18.6	17.6
Lower Arm Length: L	17.4	18.1	17.5	N/A	18.5	17.6
Arm Reach, Forward: R	32.6	32.1	32.1	N/A	34.8	31.3
Arm Reach, Forward: L	32.5	32.3	31.9	N/A	34.5	31.3
Middle Finger Length: R	3.2	3.3	3.4	3.8	3.9	2.8
Middle Finger Length: L	3.1	3.4	3.3	3.8	3.9	2.9
Hand Length: R	7.1	7.3	7.5	N/A	7.7	7.1
Hand Length: L	7.3	7.4	7.6	N/A	7.8	7.1
Hand Circumference: R	9.3	8.5	9.1	8.6	8.8	9.0
Hand Circumference: L	9.3	8.1	8.9	8.5	8.5	9.0
Hand Dominance	Right	Right	Right	Right	Right	Right

2.4 Procedure

Data were collected over a 2-week period for this project. It took approximately 8 hours to collect data from each subject. All subjects were given an initial overview and were familiarized with the LIDO Multi-Joint II system. Unsuited data were collected first. Suited tests took place 2 days later. Joints were isolated using the same posture in both the suited and unsuited conditions. Subjects were visually positioned so that the axis of the joint center was directly in line with the axis of the dynamometer shaft. Dynamometer attachments were placed to isolate the joint being measured. Subjects were then positioned and restrained to maximally stabilize the joint for strength measurements. Each subject was instructed to give a maximum effort for three repetitions through the entire range of motion (as limited by the suit and LIDO hardware). Measurements on six joint motions were taken for the suited

condition and for four different suited conditions. These four conditions were: (1) Class 1 suit with TMG; (2) Class 1 suit without TMG; (3) Class 3 suit with TMG; and (4) Class 3 suit without TMG. All testing was performed on the subject's right side while the subject was seated.

This evaluation collected concentric strength measurements where the range of motion was defined by the subject, and the angular velocity of the torque arm was held at a constant reset value by the actuator controller. Velocities selected for each joint were chosen to prevent injury (from excessive velocity) and fatigue (from too slow a velocity) to the subject. Table 2 summarizes the exercise parameters used in this investigation. While the subject was suited, gravity compensation before pressurization was performed; strength data were collected after pressurization. Because gravity compensation was needed for each joint, 24 separate pressurizations and depressurizations were required, per subject, to collect the data for six joints in each of the four suited conditions. The four suited conditions were randomized so the subjects did not receive the suited conditions in the same order.

Each trial, which encompassed three repetitions, lasted approximately 30 sec. After each trial, investigators computed a coefficient of variation for the three repetitions. This coefficient was used to determine whether there were non-maximal attempts or learning effects. If the computation was greater than 10%, the trial was repeated. After the trial was accepted, subjects were given a 5-minute rest to allow for strength recovery.

Table 2 Summary of Strength Measurement Conditions

Isolated Joint Strength Measurement	*Angular Velocity (deg/s)*
Knee Flexion/Extension	60
Wrist Flexion/Extension, Pronated	45
Shoulder Flexion/Extension	60
Shoulder Abduction/Adduction	60
Shoulder Internal/External Rotation	60
Elbow Flexion/Extension	60

A detailed description of each isolated joint strength setup appears in the following sections. Figure 6 illustrates the measured joint motions and their rotational axis coordinate systems. The terminology associated with the planes and directions relative to the human body is defined in Figure 7. These two figures, and the associated terminology, are needed to describe the procedures used to collect isolated strength data.

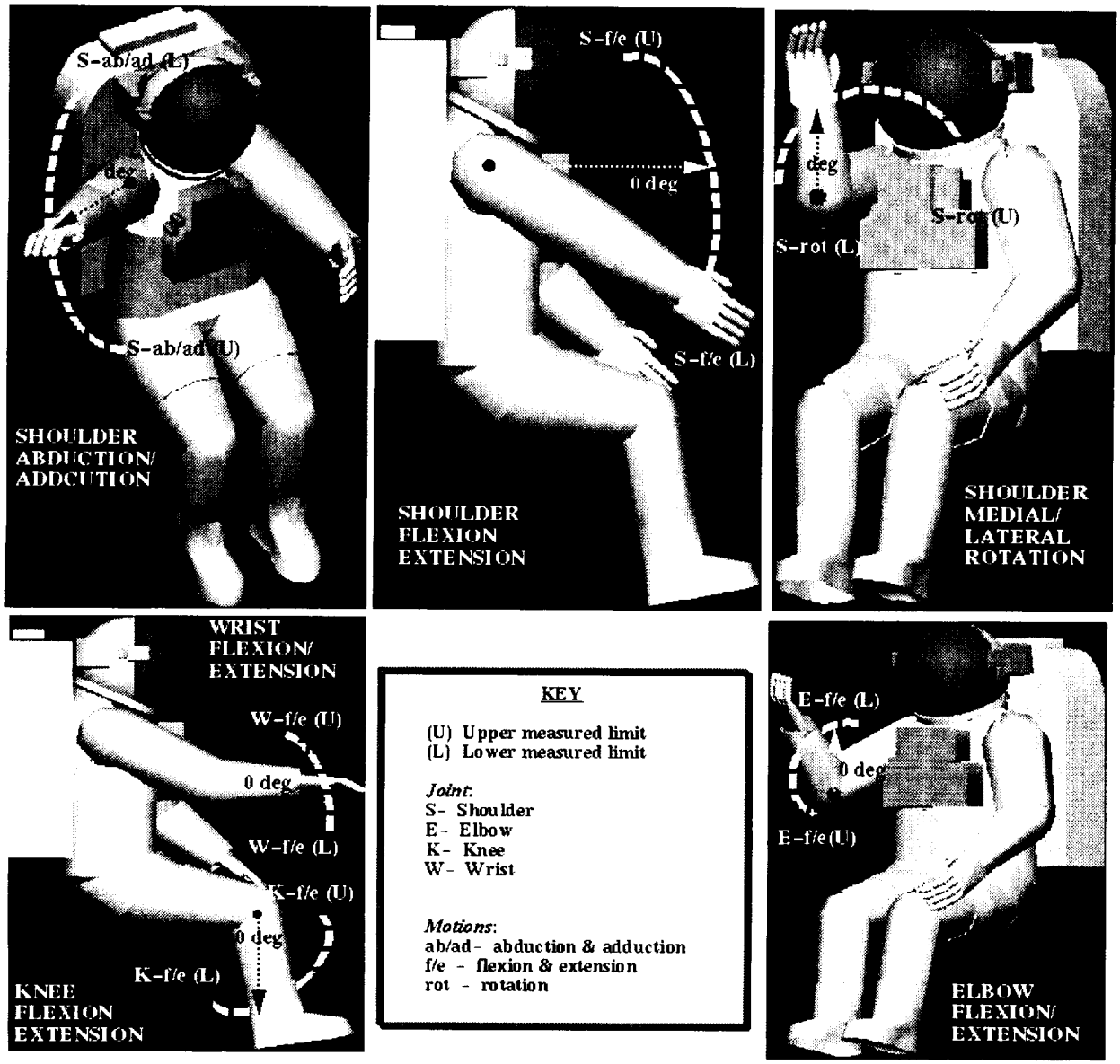

Figure 6 Illustration of the subject for each test

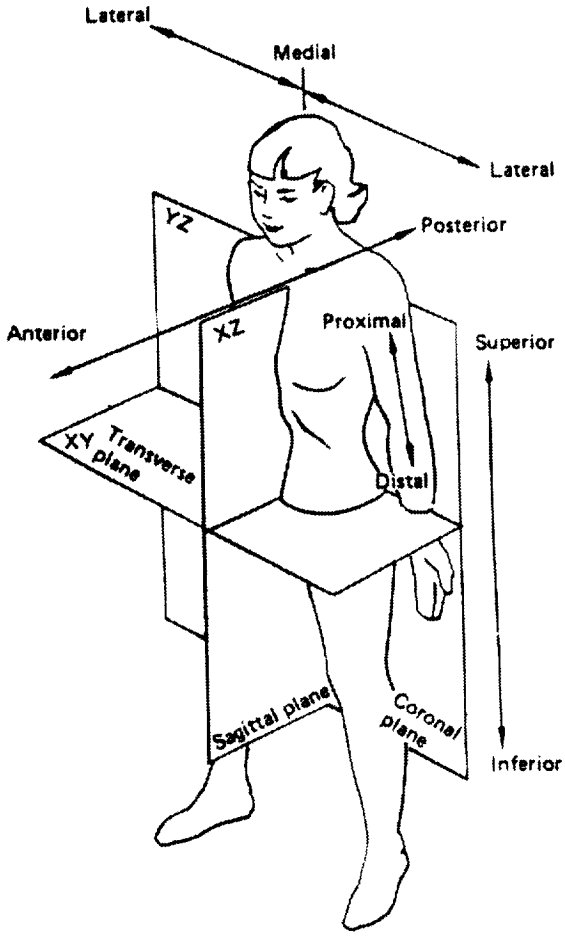

Figure 7 Body planes of motion

2.4.1 Shoulder flexion and extension

Shoulder flexion and extension were performed while the subject was in a seated position. The subject was stabilized with Velcro straps at the waist, around each thigh, and around the chest. An additional Velcro strap, which was attached to the waist strap, was placed over the subject's clavicle to further restrain the upper body (Fig. 8). The subject's entire arm was used for measurement. Thus, a hand grip became the limb attachment, and the dynamometer actuator was aligned with the subject's shoulder joint in the coronal plane of the body. The subject gripped the swivel handhold in a neutral position (no supination or pronation). Subjects were also instructed to keep their arms fully extended during the entire range of motion but not to lock their elbow joints. Once the subject was restrained on the bench, the subject's shoulder joint was placed in a neutral position (zero deg point in the range of motion), which was defined as the arm being perpendicular to the coronal plane. Since the bench was constructed with a 6-deg tilt, the subject's arm was flexed 6 deg to match the slope of the bench. Note that shoulder flexion and extension had a restricted ROM owing to interference with the bench. ROM was established by moving the subject's limb through the motion, while simultaneously comfort threshold feedback was received from the subject.

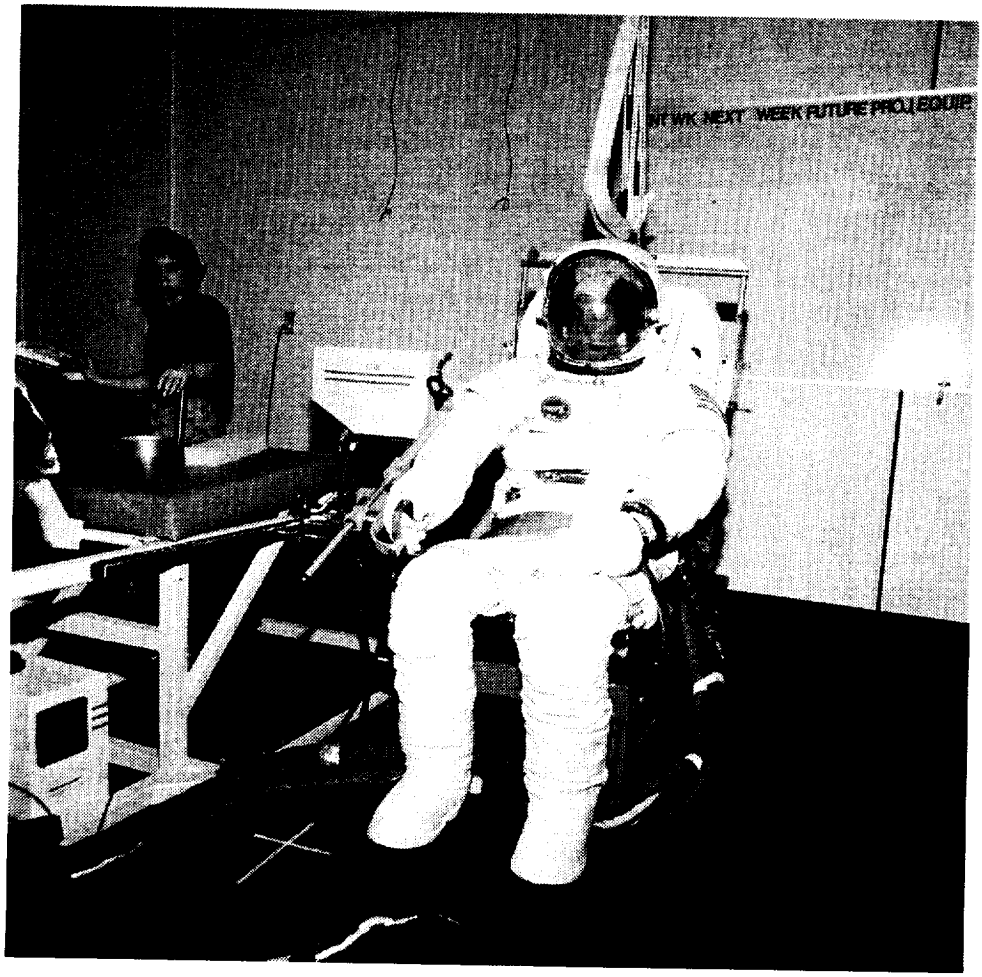

Figure 8 Shoulder flexion and extension
NASA Photo S93 32396

2.4.2 Shoulder abduction and adduction

Shoulder abduction and adduction were performed on the seated subject. Velcro straps at the waist, around each thigh, and around the chest stabilized the subject. An additional Velcro strap, which was attached to the waist strap, was placed over the subject's clavicle to further restrain the upper body (Fig. 9). Measurements were taken of the subject's entire arm. The swivel handle served as a limb attachment. The Shuttle space suit does not allow shoulder abduction and adduction in the coronal plane; therefore, the subject's arm was rotated 30 deg anterior toward the median plane. The actuator of the dynamometer system was aligned. After going posterior along the median plane and rotating it 30 deg laterally toward the subject's right arm, a 90-deg angle was achieved between the shaft of the actuator and the arm of the subject. To achieve the appropriate orientation using the seated position, the subject's legs had to straddle the base of the actuator. The subject's arm was then placed in a neutral position (zero deg point in the ROM), which is defined by the arm being perpendicular to the coronal plane. The subject's arm was raised 6 deg to match the slope of the bench. ROM was established by moving the subject's limb through the motion; comfort threshold feedback was simultaneously gotten from the subject.

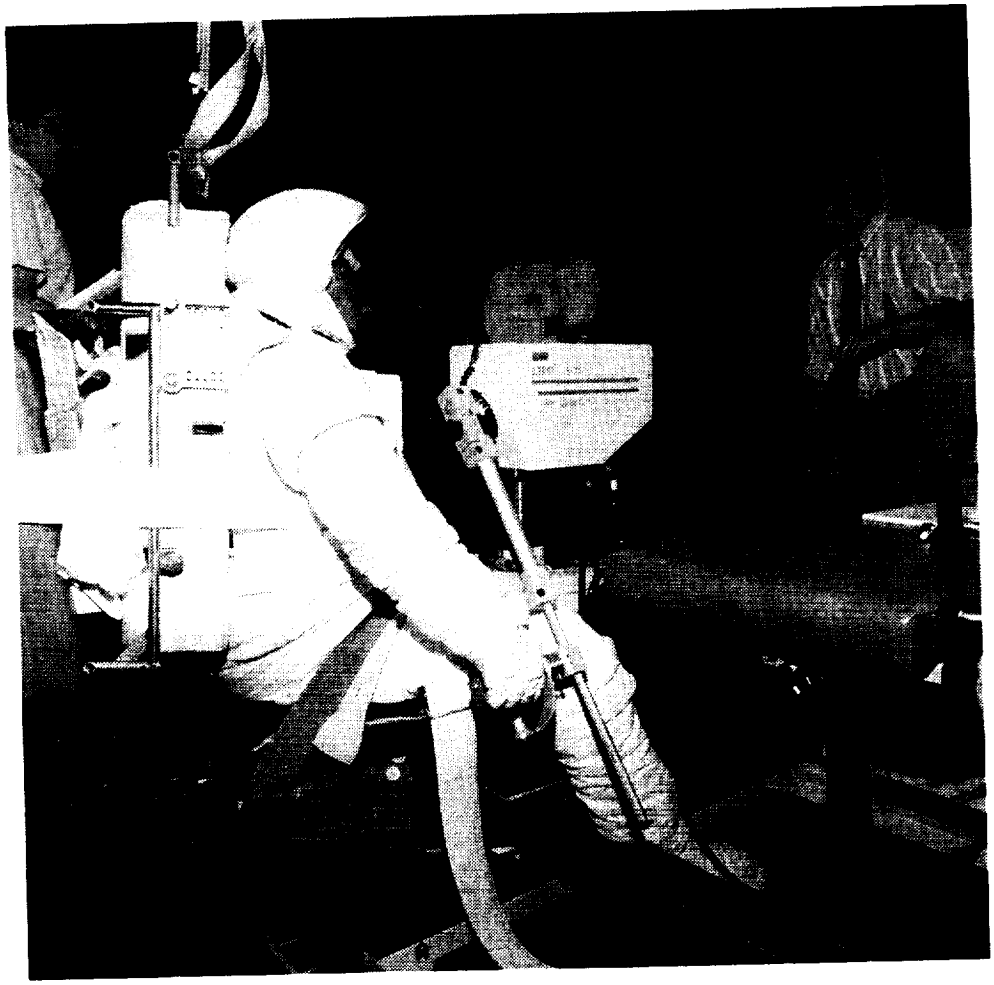

Figure 9 Shoulder abduction and adduction
NASA Photo S93 32388

2.4.3 Shoulder internal (medial) and external (lateral) rotation

During shoulder rotation, the seated subject's upper arm was positioned parallel to the coronal plane. The subject's upper arm continued parallel to the floor so that its axis of rotation would directly match the orientation of the actuator shaft. Since the bench was tilted 6 deg, the subject's shoulder joint was not perpendicular to the coronal plane. Velcro straps at the waist, around each thigh, and around the chest stabilized the subject. An additional Velcro strap was attached to the subject's waist strap and placed over the subject's clavicle to further restrain the upper body (Fig. 10). An elbow cup with Velcro straps positioned and held the distal part of the subject's upper arm in the correct position. The straight handle acted as a limit attachment at the subject's hand. The subject's arm was then placed in a neutral position (zero deg point in the ROM), which is defined as the forearm being perpendicular to the floor. ROM was established by moving the subject's arm through the motion while, simultaneously, comfort threshold feedback was received from the subject.

Figure 10 Shoulder internal (medial) and external (lateral) rotation
NASA Photo S93 32390

2.4.4 Elbow flexion and extension

For elbow flexion and extension measures, the seated subject was stabilized with Velcro straps at the waist, each thigh, and the chest. An additional Velcro strap, which was attached to the subject's waist strap, was placed over the subject's clavicle to further restrain the upper body (Fig. 11). The shoulder joint was placed in 30 deg of flexion from a position perpendicular to the coronal plane and was abducted 22.5 deg from the median plane. An elbow cup positioned and held the distal part of the subject's upper arm. Velcro straps, which were placed around the elbow cup, stabilized the subject's arm in the correct position. The straight handle was used as the limb attached at the subject's hand. The subject's arm was placed in a neutral position (zero deg point in the ROM), which is defined by the forearm being perpendicular to the floor. ROM was established by moving the subject's limb through the motion as comfort threshold feedback was received from the subject.

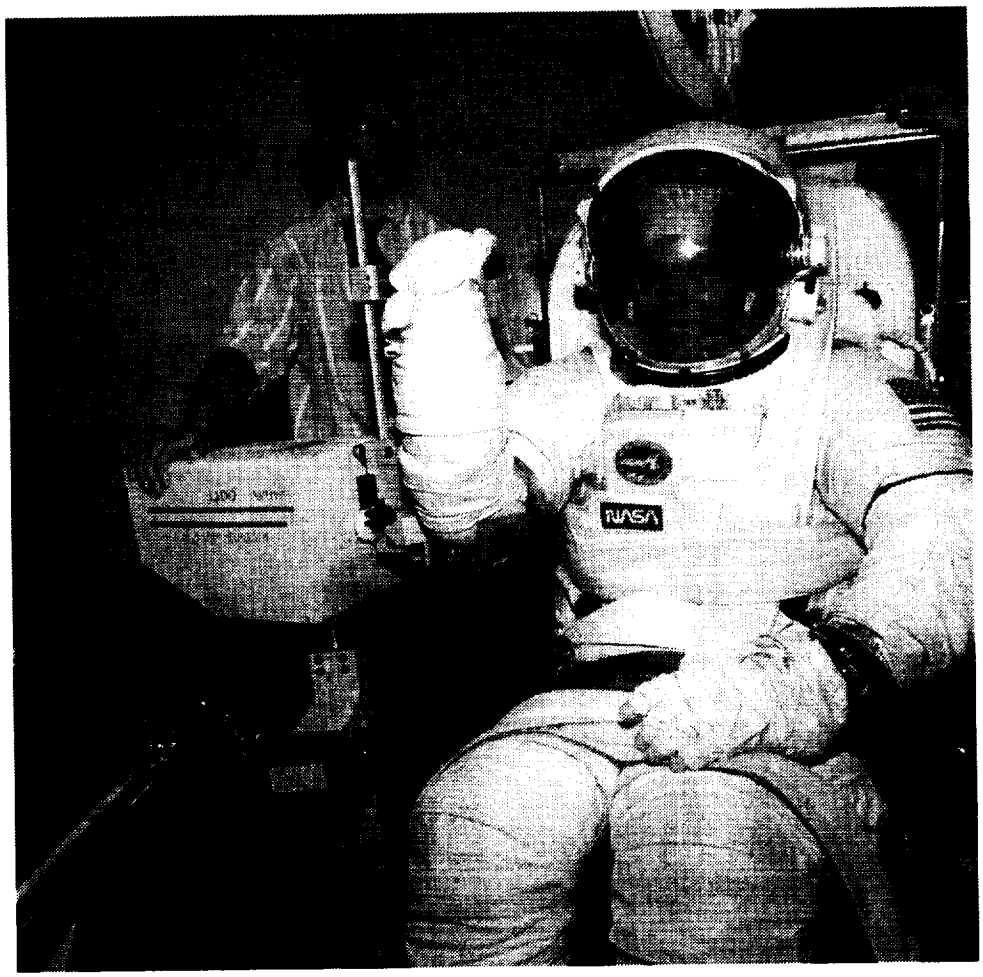

Figure 11 Elbow flexion and extension
NASA Photo S93 32400

2.4.5 Wrist flexion and extension

The subject, who was positioned in a seated posture for wrist flexion and extension, was stabilized with Velcro straps around the waist and chest. An additional Velcro strap was attached to the subject's waist strap and placed over the subject's clavicle to further restrain the upper body (Fig. 12). The subject's forearm was placed on the armrest in a horizontal position, parallel to the floor, with the subject's shoulders level. The armrest was moved so the wrist was 1.5 in. in front of the armrest. The TMG portion of the glove, which covers the glove bearing, was rolled back toward the subject's hand, and the arm was strapped down just distal to the glove bearing, under the cloth tether loop. Two Velcro straps, which were placed on the proximal end of the subject's forearm, secured the subject's arm tightly to the armrest; one was proximal to the glove bearing, and the other was on the distal end of the forearm. A handhold was placed on the left side of the subject to assist in stability, and the wrist attachment was used for the subject's hand. The subject's arm was then placed in a neutral position (zero deg point in the ROM), which is defined as the back of the hand being parallel to the floor (no flexion or extension). ROM was established by moving the subject's limb through the motion, while comfort threshold feedback was received from the subject.

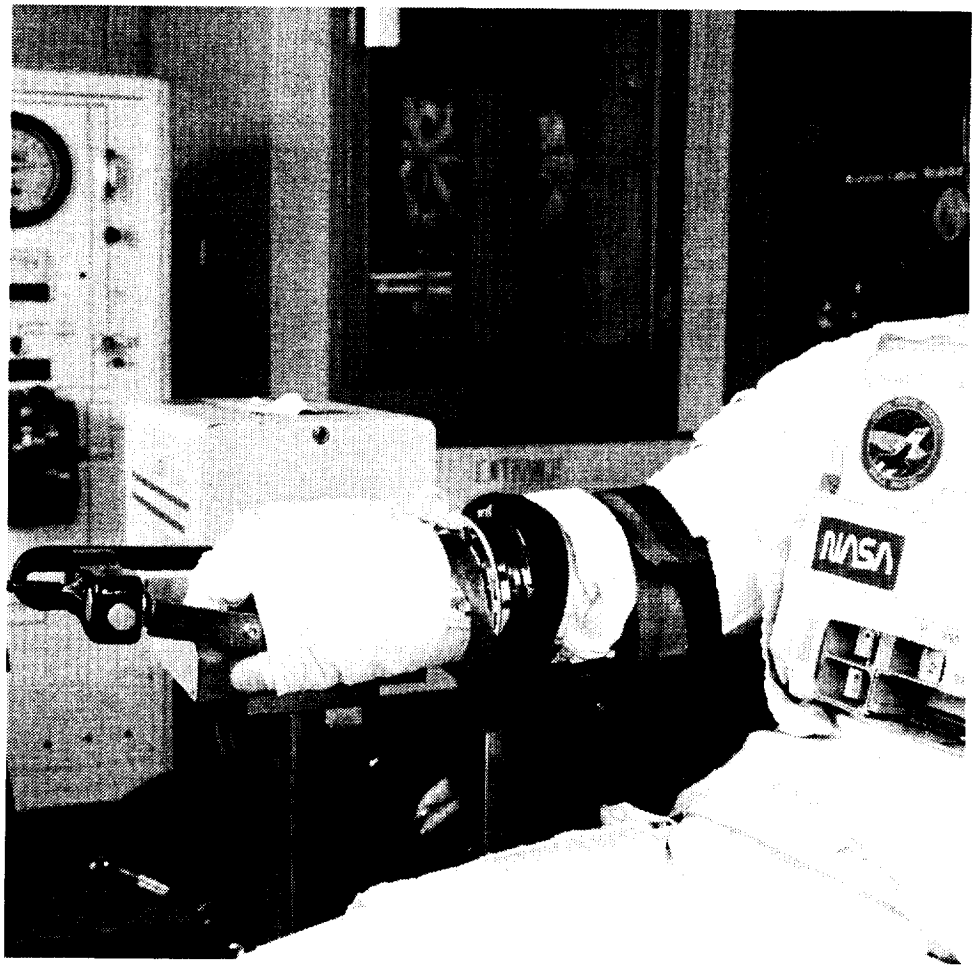

Figure 12 Wrist flexion and extension
NASA Photo S93 041608

2.4.6 Knee flexion and extension

Knee flexion and extension were performed with the subject in a seated position. Velcro straps at the waist stabilized the subject (Fig. 13). The cuff was used as the limb attachment while the dynamometer actuator was aligned with the subject's approximate knee joint center in the coronal plane. The ankle cuff was used with unsuited subjects. The thigh cuff had to be used on the ankle of suited subjects owing to the extra material of the suit. Once the subject was restrained on the bench, the subject's knee joint was placed in a neutral position (zero deg point in the ROM) defined by a 90-deg angle between the thigh and calf. Since the design of the bench places a 12-deg tilt for lower extremity measurements, the subject's calf was extended 12 deg. Note that knee flexion and extension had a limited ROM because of interference with the bench. ROM was established by moving the subject's limb through the motion while, at the same time, comfort threshold feedback was received from the subject.

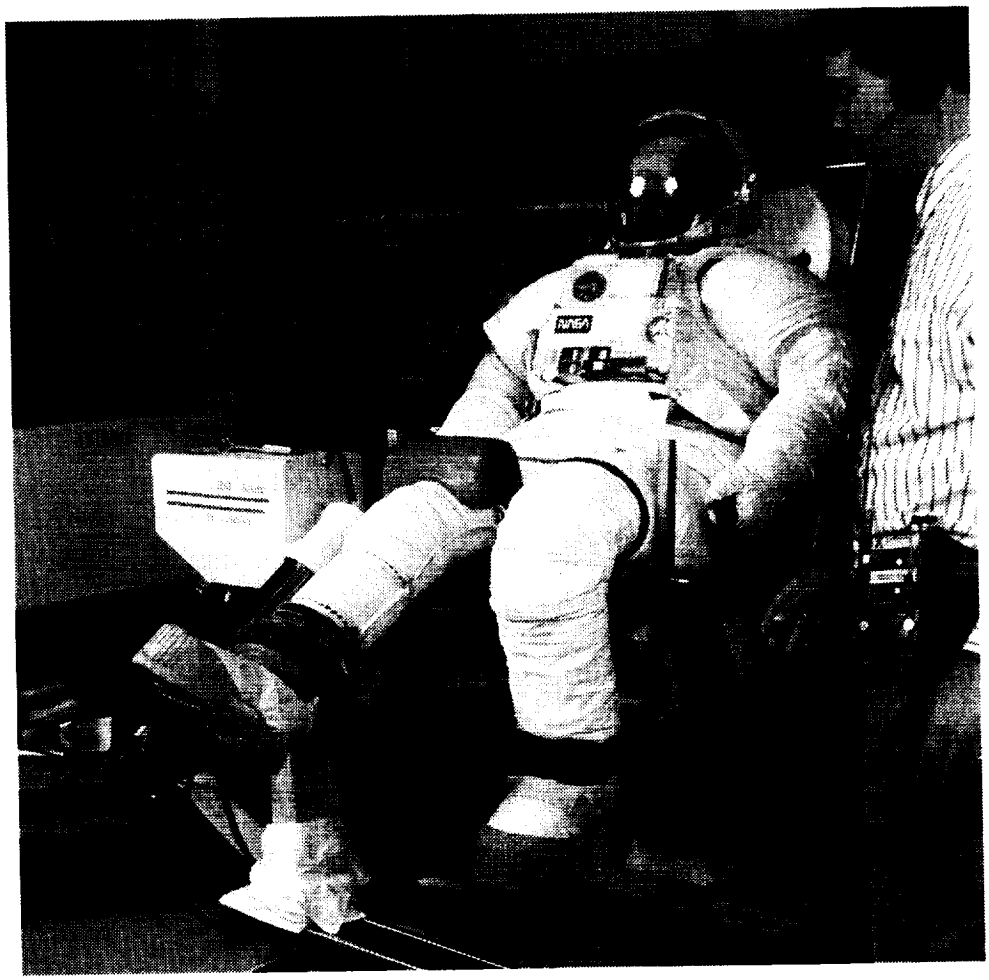

Figure 13 Knee flexion and extension
NASA Photo S93 041633

2.5 Data Processing Protocol

Figure 14 describes the data processing that was performed. A set of streamlined programs was developed to process the raw strength data produced directly by the LIDO dynamometer system. The raw data were collected using the LIDOACT software that runs on an IBM PC. Files produced on the PC were transferred to a Silicon Graphics UNIX workstation. LIDO-generated files had a main header area and several subheader areas. Lines in these areas were terminated with a linefeed as in a normal ASCII text file. The remaining data lines were terminated with a carriage return and no linefeed. Data lines were three integer values of four characters each. The first value was the corrected torque at the limb attachment (gravity compensated), the second value was the angle, and the third value was the uncorrected torque at the shift of the LIDO actuator. Corrected torque values were chosen for further processing, and a linefeed was added to each data point in the data section. This processing was done by an in-house program called 'lido'.

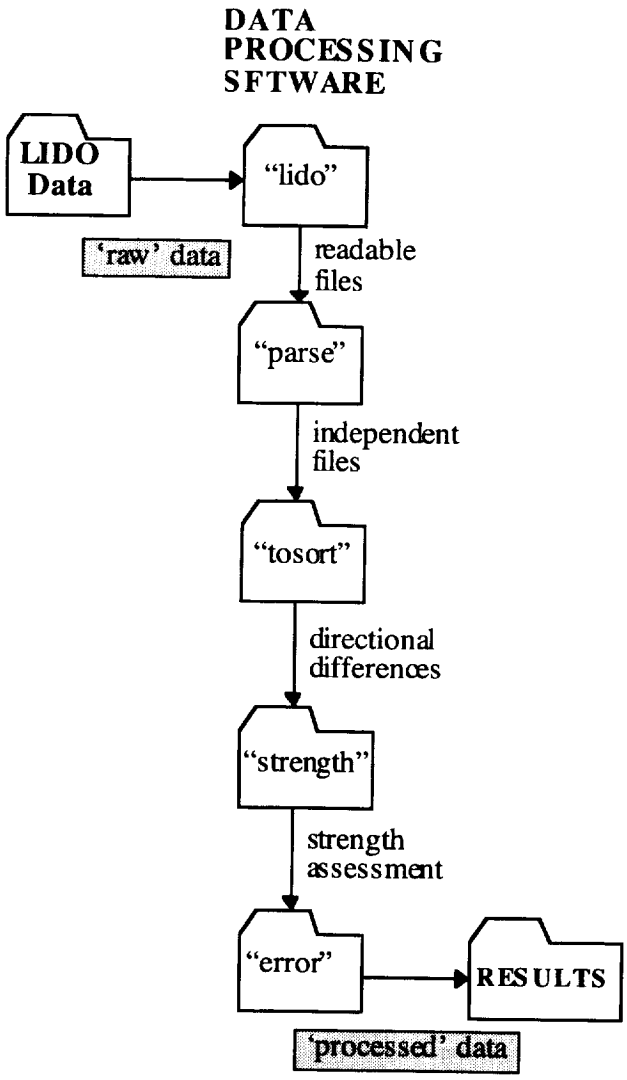

Figure 14 Isolated joint strength testing hardware and software configurations

After the corrected data were extracted and converted to a readable format, data for each subject were extracted and separated into files which had the appropriate label for suit condition using a program called 'parse'. The next step was to separate those data into opposing axes of motion (e.g., flexion and extension). The program 'tosort' was designed to accomplish this.

Because the torque data to be used by the model were to be correlated to constant velocity and maximum force, these data required filtering at extreme ranges of angular motion. The regions represented the acceleration and deceleration phases of motion performed by the subject. The acceleration phase was an increase in effort to the subject's maximum at the prescribed velocity, while the deceleration phase was an artifact created by the LIDO system to protect both subject and equipment from the rapid deceleration caused by a "hard stop." These transition regions were filtered at the beginning and ending angles by angle plots and clipping. This manual process was time consuming; but algorithmic techniques such as derivatives, jackknife residuals, leverage detection, and coefficient extraction proved ineffective in handling all variations in the data sets. Later extensions to the model might be able to accommodate these transition regions better. The operating range for data presented in this study is given in Table 3. Note that these are not anatomical ranges of motion but reference angles for the LIDO workstation, as described in sections 2.4.1 through 2.4.6.

Table 3 Operating Range for Compiled Averaged Data

Joint Motion	*Lower Bound (deg)*	*Upper Bound (deg)*
Elbow Extension	-47	31
Elbow Flexion	-35	31
Knee Extension	-57	13
Knee Flexion	-57	8
Shoulder Adduction	-31	35
Shoulder Abduction	-27	36
Shoulder Extension	-15	35
Shoulder Flexion	-16	55
Internal Shoulder Rotation	-79	11
External Shoulder Rotation	-79	0
Wrist Flexion	-14	50
Wrist Extension	-20	55

Edited torque data points were then averaged across all subjects for each joint angle, separately for each condition. A second-order polynomial regression equation of the average torque versus angle curve was calculated. Hence, all individual joint tests were reduced to a set of regression equations. This single-valued, second-order polynomial regression fitting technique was chosen for its simple and elegant form. Three polynomial coefficients are adequate to describe the torque curves. Although more exact methods of fitting are available (e.g., spline fits), it was determined that they were not needed because of the inherent error already present in the data. There is an approximately 5 to 10% variation in the data, even between the three trials of a particular joint for a given subject, so to try to fit the data to a higher resolution is unnecessary. Moreover, given a certain suit condition and joint angle, regression equations can be used for easy lookup and prediction of torques.

In the next phase of processing, differences between the unsuited and the four suited conditions were calculated and analyzed. All this data processing was computed by the in-house programs 'strength' and 'error'. The data were also partitioned into three equal ranges: A, B, and C. Partitioning was performed to try to quantify differences observed over the ROM. For instance, differences observed at one region may have been very close to unsuited values while the other regions differed significantly. Partitioning allows for a quick comparison of the regions of the ROM. For example, one possible use for regional analyses would be to assist mission planners and EVA task designers to know that a particular joint on an EVA crew member should be kept in Regions A and B, but not in Region C, for optimal strength and fatigue characteristics.

3. Results and Discussions

Data for each joint motion are graphically presented below, followed by a short summary describing each graph and table. It is important to note that the data presented here have been averaged at each angle for all six subjects. The 'Ave' condition is an average of all the suited conditions.

The following two sections (3.1 and 3.2) give an example of how to interpret the data for a single direction of one joint. The same format and techniques of analysis apply to the rest of the joint axes figures in the rest of the report.

3.1 Unsuited Conditions

This graph of suited and unsuited conditions shows three plots of torque as a function of angle: (1) unsuited torque data averaged across all six subjects, (2) second-order regression fitting the collection data, and (3) suited condition, which is averaged across all subjects and all suited conditions. The unsuited regression equation, which is listed below each unsuited summary graph, provides a very compact method of reproducing unsuited data. Figure 15 is an example of unsuited data for elbow extension, averaged for all six subjects. In each graph, averaged maximal torque is plotted versus angle for both processed unsuited data and for data predicted by the regression equation. In addition, a plot of the averaged suited condition is also presented.

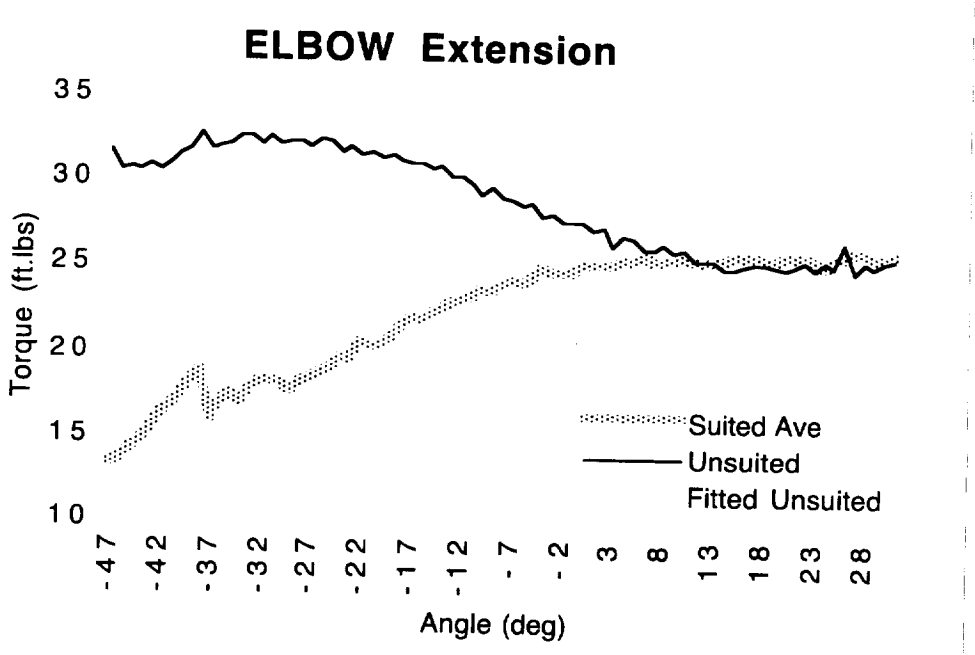

Torque Equation for Elbow Extension
Unsuited Torque = 28.166 – 0.129*angle – 0.001*angle^2

Figure 15 Unsuited and suited data for elbow extension

3.2 Comparison of Suited Versus Unsuited Conditions

Graphs and tables that show the difference between unsuited and the various suited conditions represent a complete summary of all data collected. The percentage difference between each condition relative to the unsuited condition, or baseline, is plotted for each discrete angle and averaged over the subject population. Figure 16 shows an example of the comparisons between the different suited conditions for elbow extension, plotted as a percentage change from the unsuited condition (or baseline). This figure illustrates the influence of various suits, and how they may influence the maximal torque at each angle over the data range. Also included in the analysis is a table that summarizes the average difference between each condition (Table 4). Each table is divided into thirds and labeled regions A, B, and C. This table shows the average across the whole ROM, as well as breakdowns for the three regions. Another table (Table 5) details the regression coefficients that are needed to reproduce the suited conditions relative to the unsuited condition. From these tables it is easy to estimate the average difference between any of the conditions in a region, or over the entire data set.

For example, the first column of data in Table 4 represents the percent change for each of the suited conditions and average (Ave) with respect to the unsuited condition (ux). From this line, it can be noted that there is a 21% reduction in force for the average, a 29% decrease in force for 3t, a 25% decrease for 3u, a 12% decrease for 1t, and an 18% decrease for 1u, all with respect to the unsuited condition. It is thus possible to compare any two conditions within any region.

In certain situations (i.e., modeling of EMU strength), it is convenient to estimate suited strength data from unsuited strength data. For elbow extension, Table 5 represents the conversion coefficients that allow this estimation. If the estimated torque for a particular angle under a specific suited condition is desired, the unsuited torque at that angle can be used in conjunction with regression coefficients from this table. For example, if the torque of an unsuited subject is known, the estimated suited torque can be derived by adding the percent change from the unsuited condition. The appropriate regression equation from Table 5 was evaluated to derive the torque at –17 deg for 3u.

$$-11.31 + 0.86*angle - 0.01*angle^2$$

(at –17 deg, the answer is –26.2%)

This value represents the percent degradation from the unsuited condition. This method can be used to obtain torque estimates for any suited condition and for the unsuited average. If calculated over the whole operating range, torque curves for any condition can be reproduced.

3.3 Elbow Extension

In the *unsuited condition*, torques averaged approximately 28 ft-lb. The little variance in data resulted in the regression equation fitting very well (Fig. 15). The overall trend seen in the unsuited condition was a higher torque at the more negative angle, or flexed elbow. It is also clear that the average suited condition was consistently lower from –47 to 13 deg, on average 21% degraded, than the unsuited torque with a steep upward slope.

In comparing the *suited conditions* to the unsuited baseline (Fig. 16) and Table 4, 1u was closest overall (an 18% average decrease in maximal torque from the unsuited), while the farthest was the 3t condition (–29%). Although 1t had a higher differential average than 1u (–12 vs. –18%), this was believed to result from erroneous data points at the very beginning of the graph. Overall, the average of all suited conditions was –21% from the unsuited condition. It is plainly seen from the graph that the higher angle of extension (more negative angles) had substantially decreased maximal torque ability.

With the exception of the 1t condition, all suited conditions lie very close to one another, as can be seen both from the graph and from the regional average tables. Most averages, other than those for 1t and some few exceptions, differed within 10% of each other. In each region, 1u was closest to the unsuited condition, and 3t was farthest from the unsuited condition.

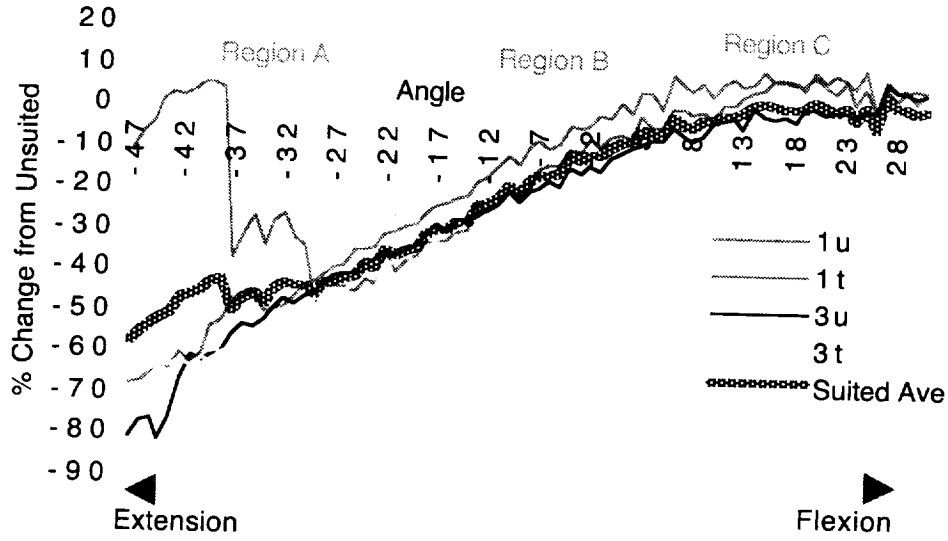

Figure 16 Comparisons of suited conditions

Table 4 Suited Comparisons

Joint: ELBOW Extension
Differences in % Change from Unsuited
****

TOTAL ROM (filtered) <-47 to 31>

	ux	*1u*	*1t*	*3u*	*3t*
Ave	-21	-3	-8	3	8
3t	-29	-11	-17	-4	
3u	-25	-6	-12		
1t	-12	5			
1u	-18				

REGION A <-47 to -21>

	ux	*1u*	*1t*	*3u*	*3t*
Ave	-45	4	-22	9	9
3t	-54	-4	-31	0	
3u	-55	-5	-32		
1t	-22	26			
1u	-49				

REGION B <-21 to 5>

	ux	*1u*	*1t*	*3u*	*3t*
Ave	-19	-7	0	1	5
3t	-24	-12	-5	-3	
3u	-20	-8	-1		
1t	-19	-7			
1u	-12				

REGION C <5 to 31>

	ux	*1u*	*1t*	*3u*	*3t*
Ave	0	-6	-4	0	9
3t	-9	-16	-13	-9	
3u	0	-7	-4		
1t	4	-2			
1u	6				

Table 5 Regression Coefficients

Difference Coefficients, from Unsuited
% Change = B_0 + B_1* angle + B_2* angle^2

	B_0	B_1	B_2
1u:	-3.23	0.83	-0.01
1t:	-16.78	0.74	0.02
3u:	-11.31	0.86	-0.01
3t:	-17.32	0.65	-0.01
Ave:	-12.16	0.77	0.00

Legend:

ux	unsuited
1u	Class 1 suit, no TMG
1t	Class 1 suit with TMG
3u	Class 3 suit, no TMG
3t	Class 3 suit with TMG
Ave	Average of all four suited conditions

3.4 Elbow Flexion

In *unsuited* elbow flexion, the torque averaged about 29 ft-lb (Fig. 17). This was very similar to elbow extension. The torques tended to decrease with a larger angle of flexion with little variation in data, which resulted in a regression curve similar to the extension case. The average of the suited data differed most at negative angles, but for the whole ROM it was only 11% degraded from the unsuited condition.

Differences in all *suited conditions* were not as drastic as those for elbow extension (Fig. 18). The closest average to the unsuited condition over the whole ROM, which ranged from a 30% reduction to a small increase in maximal torques, was that of 1t (an 8% reduction). The farthest average from the baseline was 3t (a 16% decrease). Overall, however, the total reduction was not as great as elbow extension, though the graphs of the individual conditions were similar – within about 10% of each other.

Region A was the area that differed most from the unsuited baseline torques; it started out with an average difference of –19%. As the motion moved into Regions B and C, averages became –7%. In Region C, a separation was apparent at the end of the motion where 1t and 1u rose to match the baseline and 3t and 3u decreased.

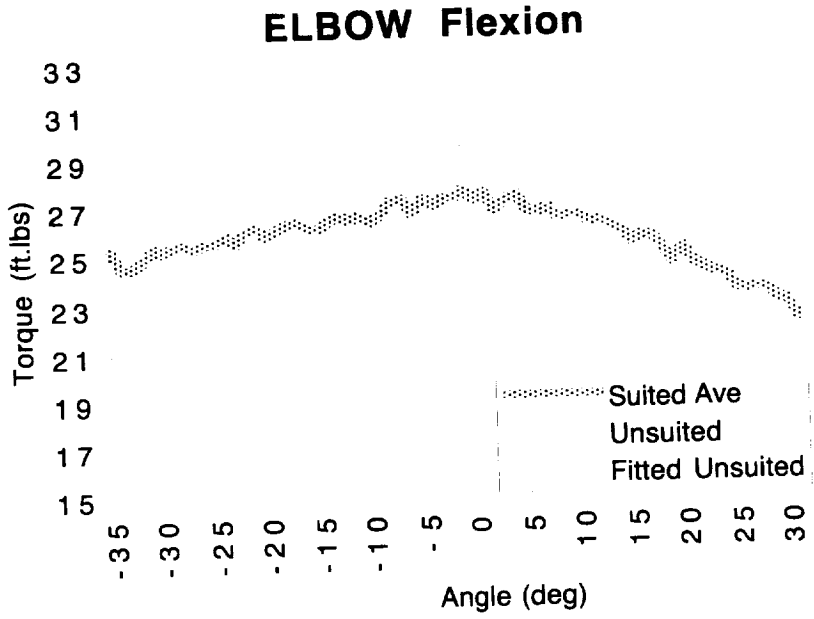

Torque Equation for Elbow Flexion
Unsuited Torque = 29.326 – 0.117*angle – 0.001*angle^2

Figure 17 Unsuited data for elbow flexion

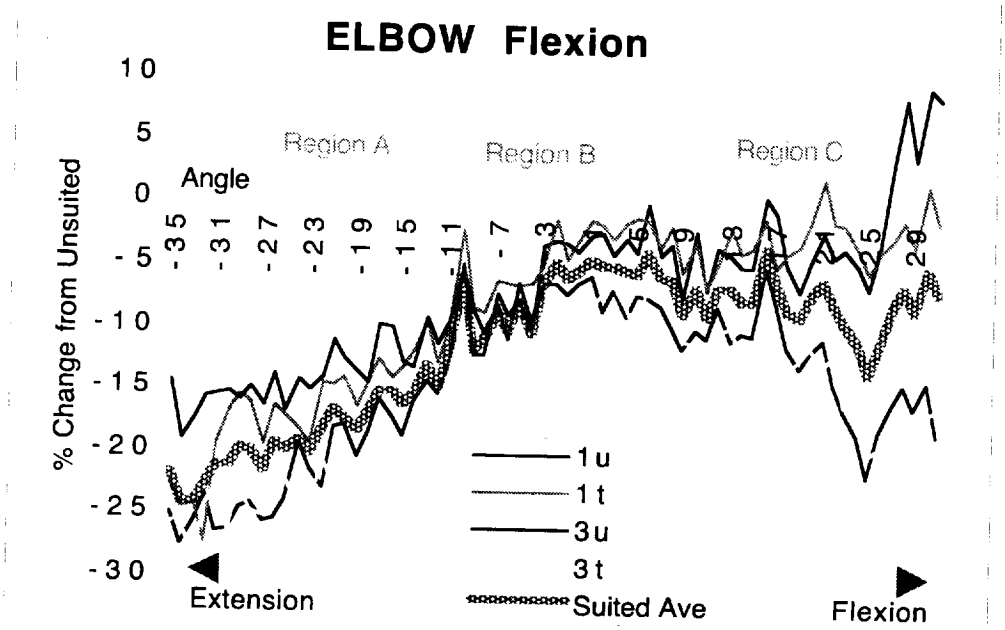

Joint: ELBOW Flexion
Differences in % Change from Unsuited
****

TOTAL ROM (filtered) <-35 to 31>

	ux	*1u*	*1t*	*3u*	*3t*
Ave	-11	-1	-3	0	4
3t	-16	-6	-7	-4	
3u	-11	-1	-3		
1t	-8	1			
1u	-10				

REGION A <-35 to -13>

	ux	*1u*	*1t*	*3u*	*3t*
Ave	-19	2	-1	-4	4
3t	-23	-1	-5	-9	
3u	-14	7	3		
1t	-17	4			
1u	-22				

REGION B <-13 to 9>

	ux	*1u*	*1t*	*3u*	*3t*
Ave	-7	-1	-2	0	3
3t	-11	-4	-6	-3	
3u	-8	-1	-3		
1t	-4	1			
1u	-6				

REGION C <9 to 31>

	ux	*1u*	*1t*	*3u*	*3t*
Ave	-7	-5	-5	4	5
3t	-13	-11	-10	0	
3u	-12	-10	-9		
1t	-2	0			
1u	-2				

Difference Coefficients, from Unsuited
% Change = B_0 + B_1* angle + B_2* angle^2

	B_0	B_1	B_2
1u:	-7.18	0.44	-0.01
1t:	-4.87	0.30	-0.01
3u:	-8.39	-0.02	-0.01
3t:	-11.62	0.16	-0.01
Ave:	-8.01	0.22	-0.01

Legend:

ux	unsuited
1u	Class 1 suit, no TMG
1t	Class 1 suit with TMG
3u	Class 3 suit, no TMG
3t	Class 3 suit with TMG
Ave	Average of all four suited conditions

Figure 18 Suited data for elbow flexion

3.5 Knee Extension

Unsuited knee extension produced an average torque of approximately 110 ft-lb, with maximum and minimum torques of 140 and 88 ft-lb, respectively (Fig. 19). In the ROM, the torque increased from –57 deg until about 22 deg. At 22 deg it began to decrease until motion reached the limits. The suited average condition followed an almost identical trend, but overall was degraded by approximately 5%. Characteristics of the suit for knee extension did not seem to impede the knee extension very much because the magnitude and shape of the torque curve were very similar to those of the unsuited condition.

Overall, the *suited* percentage difference graphs were linear and very tightly grouped (Fig. 20). The steady increase in strength as the angle increased indicated less of a drop off of maximal strength when compared to the unsuited condition. The average across the ROM of the averaged (Ave) suited condition was very similar to the unsuited baseline because the data rose linearly from below –10% in the beginning to above 10% at the end.

A large data point at the end of 3t could have influenced the average. Regression equations for this motion indicate that any suited condition can be estimated by linear coefficients, as observed by the zero-valued coefficients in the B_2 column.

Region A was the least similar to the unsuited baseline, with its average of suited conditions falling at –10%. Also, the most divergence seemed apparent in this region. All the graphs in Region B were very tightly aligned, and the maximal torque continued to rise towards the unsuited condition through Regions B and C. Region C shows graphs that had increased torques slightly over the baseline.

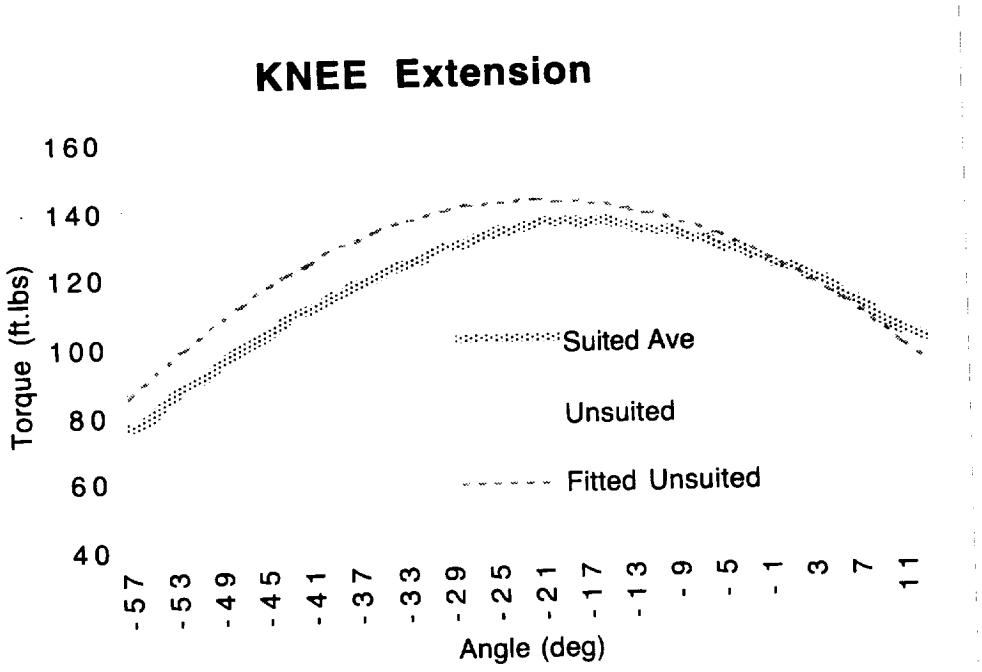

Torque Equation for Knee Extension
Unsuited Torque = 122.158 – 1.801*angle – 0.043*angle^2

Figure 19 Unsuited data for knee extension

KNEE Extension

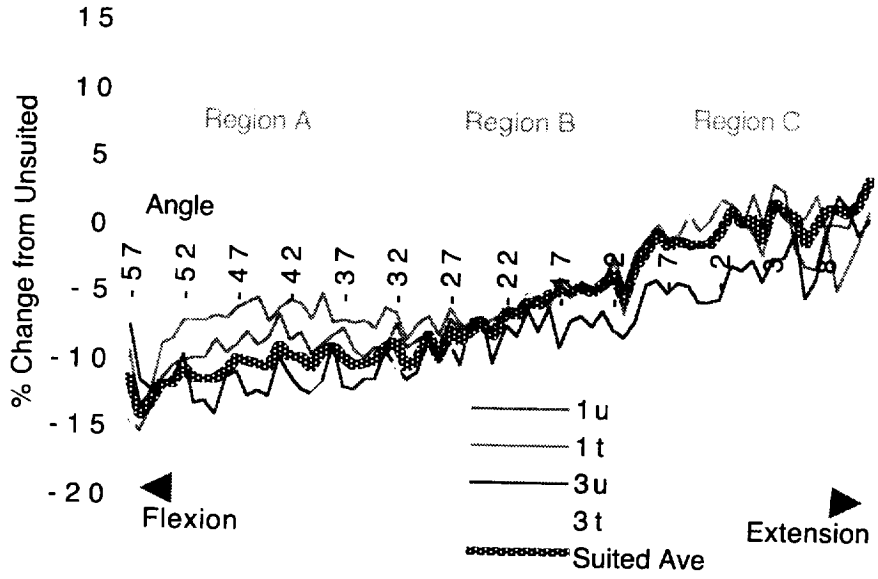

Joint: KNEE Extension
Differences in % Change from Unsuited
****

TOTAL ROM (filtered) <-57 to 13>

	ux	*1u*	*1t*	*3u*	*3t*
Ave	-5	0	-1	1	0
3t	-5	0	0	2	
3u	-7	-2	-2		
1t	-4	0			
1u	-4				

REGION A <-57 to -34>

	ux	*1u*	*1t*	*3u*	*3t*
Ave	-10	0	-3	0	3
3t	-14	-4	-6	-2	
3u	-11	-1	-4		
1t	-7	2			
1u	-9				

REGION B <-34 to -10>

	ux	*1u*	*1t*	*3u*	*3t*
Ave	-6	0	0	1	0
3t	-6	0	0	1	
3u	-8	-1	-2		
1t	-5	0			
1u	-6				

REGION C <-10 to 13>

	ux	*1u*	*1t*	*3u*	*3t*
Ave	0	0	0	3	-3
3t	3	3	3	6	
3u	-2	-3	-2		
1t	0	0			
1u	0				

Difference Coefficients, from Unsuited
% Change = B_0 + B_1* angle + B_2* angle^2

	B_0	B_1	B_2
1u:	0.62	0.33	0.00
1t:	-0.21	0.27	0.00
3u:	-2.37	0.37	0.00
3t:	3.95	0.55	0.00
Ave:	0.50	0.38	0.00

Legend:

ux	unsuited
1u	Class 1 suit, no TMG
1t	Class 1 suit with TMG
3u	Class 3 suit, no TMG
3t	Class 3 suit with TMG
Ave	Average of all four suited conditions

Figure 20 Suited data for knee extension

3.6 Knee Flexion

For the *unsuited condition*, the torques started at 70 ft-lb. From 42 deg to the end of the ROM, these torques decreased evenly, ending at about 50 ft-lb (Fig. 21). The average suited condition follows the same trend but is degraded by an average of 5% from the unsuited condition.

The averages of the *suited conditions* were nearly the same as those for the unsuited conditions; however, there was a strong linear decrease over the whole ROM (Fig. 22). All conditions were within 7% of each other. Many comparisons yielded a zero average difference. The suited data for knee extension resulted in an opposite slope than that for knee flexion. Regression equations for this motion suggest that any suited condition may be easily estimated by linear coefficients.

Region A, which is where all graphs were very closely grouped, started off 10% above the unsuited condition. Region B was where the graphs were most diverse, but all were still within 8% of each other; most were within 3% of each other. The closest to baseline and the most distinct in this region was 1u.

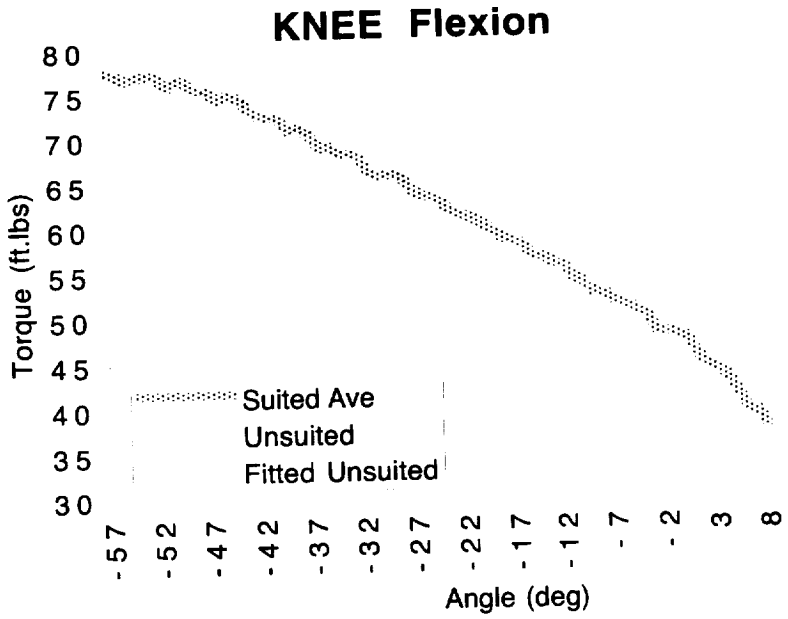

Torque Equation for Knee Flexion
Unsuited Torque = 54.34 – 0.658*angle – 0.0006*angle^2

Figure 21 Unsuited data for knee flexion

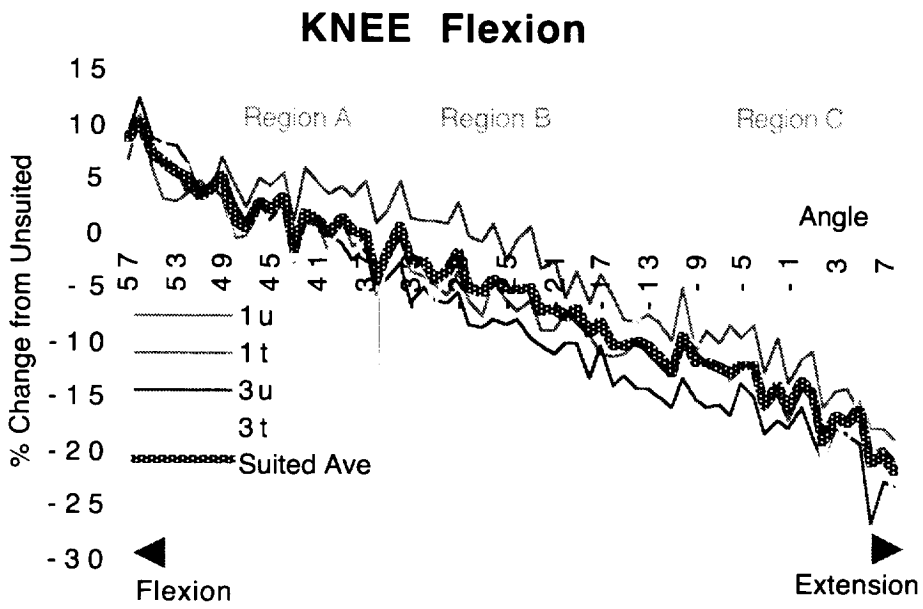

Joint: KNEE Flexion
Differences in % Change from Unsuited
****
TOTAL ROM (filtered) <-57 to 8>

	ux	*1u*	*1t*	*3u*	*3t*
Ave	-5	-2	0	2	0
3t	-5	-2	0	1	
3u	-7	-4	-1		
1t	-6	-3			
1u	-2				

REGION A <-57 to -35>

	ux	*1u*	*1t*	*3u*	*3t*
Ave	2	-1	0	0	1
3t	1	-2	0	-1	
3u	3	-1	1		
1t	1	-2			
1u	4				

REGION B <-35 to -14>

	ux	*1u*	*1t*	*3u*	*3t*
Ave	-5	-3	1	3	0
3t	-5	-3	1	3	
3u	-8	-7	-2		
1t	-6	-5			
1u	-1				

REGION C <-14 to 8>

	ux	*1u*	*1t*	*3u*	*3t*
Ave	-14	-2	0	2	0
3t	-14	-2	0	2	
3u	-17	-5	-3		
1t	-14	-2			
1u	-12				

Difference Coefficients, from Unsuited
% Change = B_0 + B_1* angle + B_2* angle^2

	B_0	B_1	B_2
1u:	-13.55	-0.60	0.00
1t:	-15.30	-0.32	0.00
3u:	-18.71	-0.34	0.00
3t:	-15.75	-0.45	0.00
Ave:	-15.83	-0.43	0.00

Legend:

ux	unsuited
1u	Class 1 suit, no TMG
1t	Class 1 suit with TMG
3u	Class 3 suit, no TMG
3t	Class 3 suit with TMG
Ave	Average of all four suited conditions

Figure 22 Suited data for knee flexion

3.7 Shoulder Adduction

Unsuited data for shoulder adduction show that the torques changed little as the angle changed (Fig. 23). Starting at 45 ft-lb, the data dropped slightly to 41 ft-lb before increasing again to 43 ft-lb at the end of the ROM. The suited average differed vastly (about –40%) at the more negative angles and rose up to –13% at the positive angles.

Because the Class 3 suit was unavailable, the two *suited conditions*, 1u and 1t, were the only conditions examined for all shoulder motions. In comparing suited conditions (Fig. 24), it could be seen that maximal torques rose significantly as the angle increased. The curves had a steep slope that started out at 40 to 50% below the unsuited condition and converged to zero difference from the unsuited condition. Regression equations show that these graphs can be obtained using a linear estimation.

Regions A and B were the most diverse of the three regions. The 1u condition averaged 7 to 9% closer to the unsuited data than the 1t condition. Data overlapped in Region C as the torques approached those of unsuited magnitude.

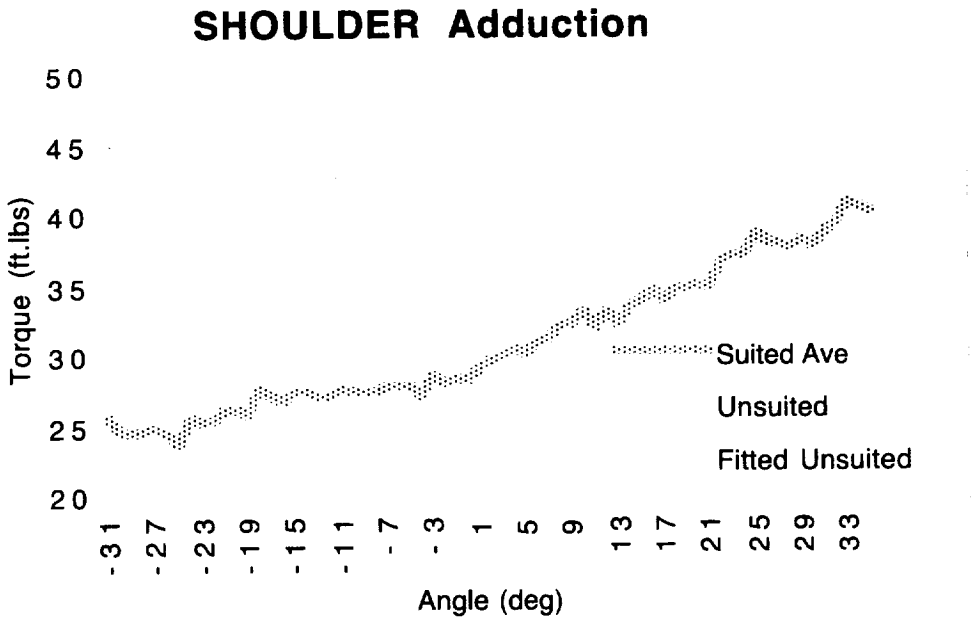

Torque Equation for Shoulder Adduction
Unsuited Torque = 41.933 – 0.037*angle + 0.002*angle^2

Figure 23 Unsuited data for shoulder adduction

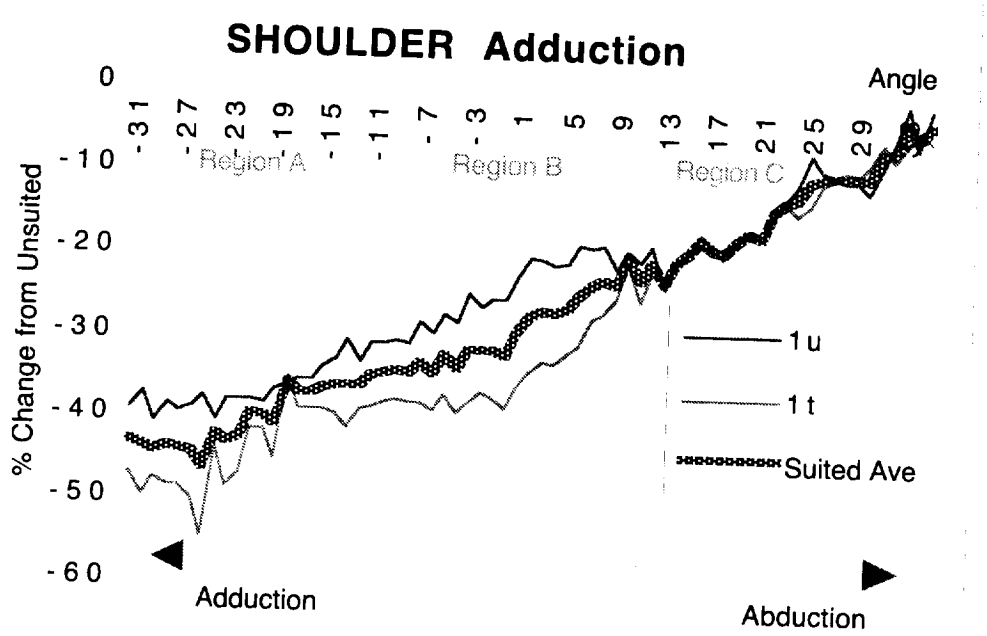

Joint: SHOULDER Adduction
Differences in % Change from Unsuited
****

TOTAL ROM (filtered) <-31 to 35>

	ux	*lu*	*lt*
Ave	-27	-2	2
lt	-29	-5	
lu	-24		

REGION A <-31 to -9>

	ux	*lu*	*lt*
Ave	-40	-3	3
lt	-43	-7	
lu	-36		

REGION B <-9 to 13>

	ux	*lu*	*lt*
Ave	-28	-4	4
lt	-33	-9	
lu	-23		

REGION C <13 to 35>

	ux	*lu*	*lt*
Ave	-13	0	0
lt	-13	0	
lu	-13		

Difference Coefficients, from Unsuited
% Change = B_0 + B_1* angle + B_2* angle^2

	B_0	B_1	B_2
lu:	-25.94	0.54	0.00
lt:	-33.36	0.68	0.01
Ave:	-29.65	0.61	0.00

Legend:

ux	unsuited
lu	Class 1 suit, no TMG
lt	Class 1 suit with TMG
Ave	Average of both suited conditions

Figure 24 Suited data for shoulder adduction

3.8 Shoulder Abduction

Unsuited data were lower in maximal torque that those of shoulder adduction (Fig. 25). The torques, which peaked at 32 ft-lb, reduced to about 27 ft-lb over the course of motion. The suited average followed the same trend but was, on average, 18% degraded.

Percentage difference plots showed a similar trend, but a different torque magnitude, for *suited conditions* (Fig. 26). Condition 1t was very similar to the unsuited condition for the more negative angles, whereas condition 1u remained near a 30% decrease through the whole range.

Region A showed that 1t was very similar to the baseline and that 1u had a 37% average reduction in maximal torque. Condition 1t was very flat in this region, but condition 1u slightly increased. In Region B, condition 1t dropped below the baseline, and condition 1u flattened out at –26%. The graphs were closest to each other and were decreasing in Region C.

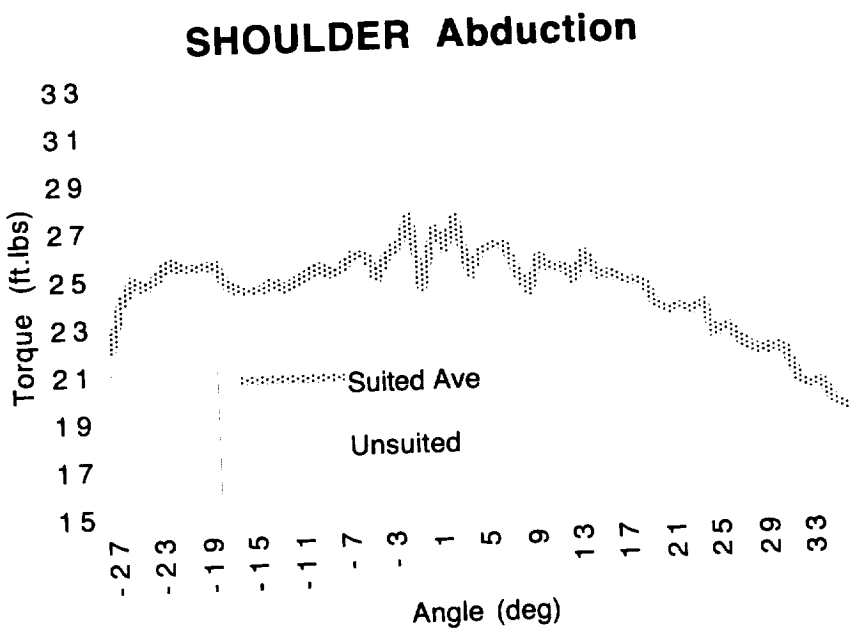

Torque Equation for Shoulder Abduction
Unsuited Torque = 30.094 – 0.058*angle – 0.001*angle^2

Figure 25 Unsuited data for shoulder abduction

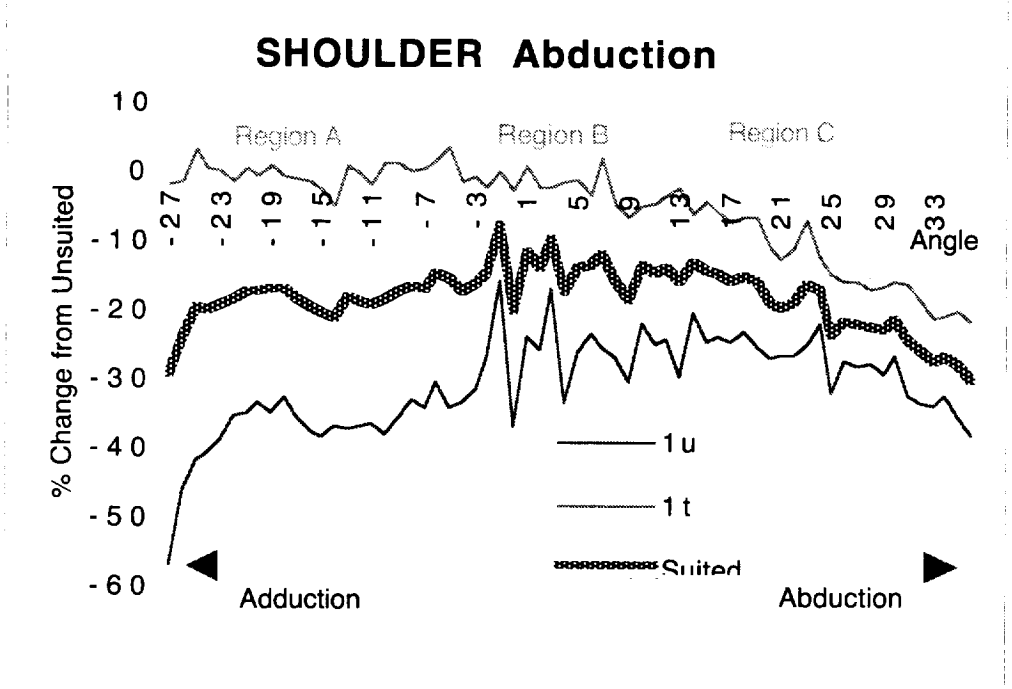

Joint: SHOULDER Abduction
Differences in % Change from Unsuited
****

TOTAL ROM (filtered) <-27 to 36>

	ux	*lu*	*lt*
Ave	-18	12	-12
lt	-5	25	
lu	-31		

REGION A <-27 to -6>

	ux	*lu*	*lt*
Ave	-19	18	-18
lt	0	37	
lu	-37		

REGION B <-6 to 15>

	ux	*lu*	*lt*
Ave	-14	12	-12
lt	-2	24	
lu	-26		

REGION C <15 to 36>

	ux	*lu*	*lt*
Ave	-20	7	-7
lt	-13	14	
lu	-27		

Difference Coefficients, from Unsuited
% Change = B_0 + B_1* angle + B_2* angle^2

	B_0	B_1	B_2
lu:	-27.42	0.33	-0.01
lt:	-0.85	-0.23	-0.01
Ave:	-14.13	0.05	-0.01

Legend:

ux	unsuited
1u	Class 1 suit, no TMG
1t	Class 1 suit with TMG
Ave	Average of both suited conditions

Figure 26 Suited data for shoulder abduction

3.9 Shoulder Extension

The *unsuited conditions* showed that the data fit well to a near-linear regression (Fig. 27). Additionally, torques did not change much over the range which began at 53 ft-lb and rose to 58 ft-lb. The suited average condition differed most at the negative angles and averaged 42% lower than the unsuited condition.

The two *suited conditions*, 1u and 1t, were extremely similar to each other along the entire range (Fig. 28) because they rose from a 60% reduction in available torque to about a 30% reduction. The average for the range was 42% degraded from the unsuited condition. Regression equations for both conditions and the average showed that all plots can be represented by a linear regression.

Region A showed very little difference between the two data sets. The data sets diverged slightly in Regions B and C, and ended about 6% different at the final position.

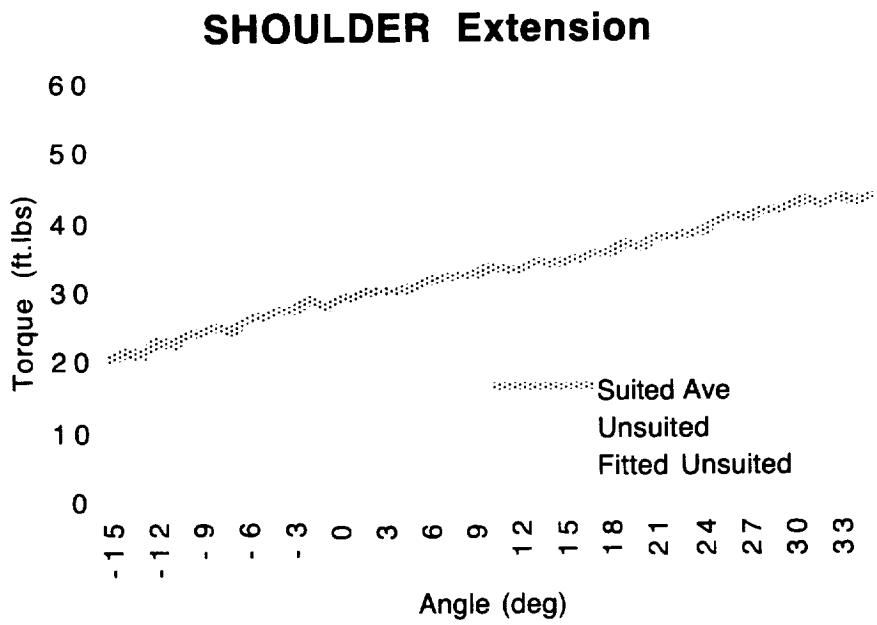

Torque Equation for Shoulder Extension
Unsuited Torque = 56.569 + 0.101*angle – 0.002*angle^2

Figure 27 Unsuited data for shoulder extension

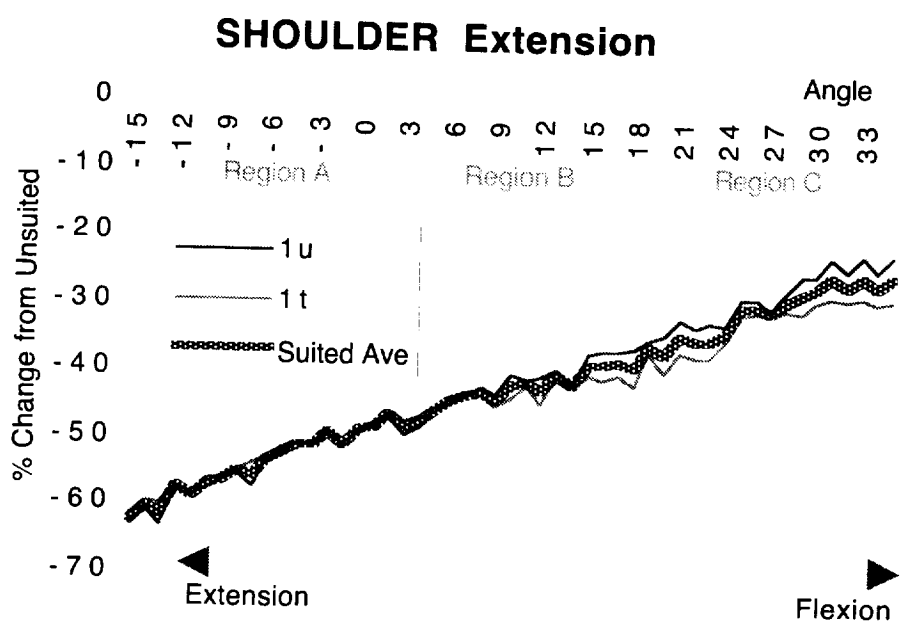

Joint: SHOULDER Extension
Differences in % Change from Unsuited
****

TOTAL ROM (filtered) <-15 to 35>

	ux	*lu*	*lt*
Ave	-42	0	0
lt	-43	-1	
lu	-42		

REGION A <-15 to 2>

	ux	*lu*	*lt*
Ave	-54	0	0
lt	-54	0	
lu	-55		

REGION B <2 to 18>

	ux	*lu*	*lt*
Ave	-43	0	0
lt	-43	-1	
lu	-42		

REGION C <18 to 35>

	ux	*lu*	*lt*
Ave	-30	-1	1
lt	-32	-3	
lu	-28		

Difference Coefficients, from Unsuited
% Change = B_0 + B_1* angle + B_2* angle^2

	B_0	B_1	B_2
lu:	-49.92	0.79	0.00
lt:	-49.93	0.66	0.00
Ave:	-49.92	0.72	0.00

Legend:

ux	unsuited
1u	Class 1 suit, no TMG
1t	Class 1 suit with TMG
Ave	Average of both suited conditions

Figure 28 Suited data for shoulder extension

3.10 Shoulder Flexion

Shoulder flexion was lower in magnitude than shoulder extension in the *unsuited condition*. The torques decreased as the angle increased from 42 to about 30 ft-lb (Fig. 29). The suited average, which followed the same trend, averaged 42% lower.

In the *suited conditions* (Fig. 30) the two conditions, 1u and 1t, differed little. Overall they averaged within 3% of each other.

Data in Region A were the closest in magnitude. Regions B and C had the greatest variation. The end portion of Region C showed an unusual fluctuation.

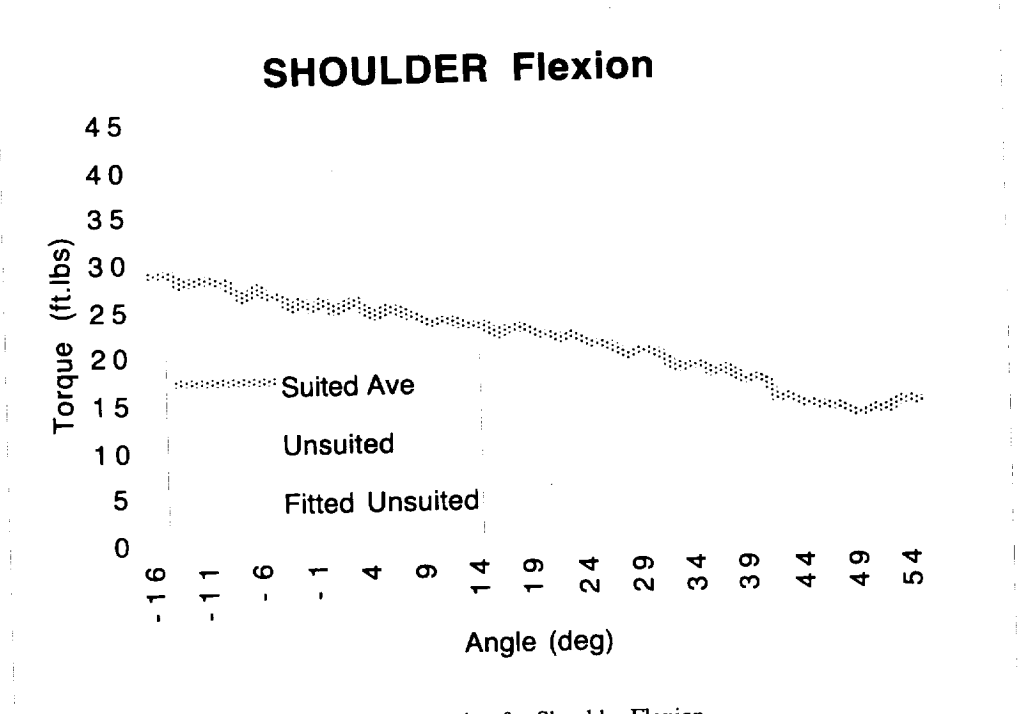

Torque Equation for Shoulder Flexion
Unsuited Torque = 39.714 - 0.131*angle - 0.001*angle^2

Figure 29 Unsuited data for shoulder flexion

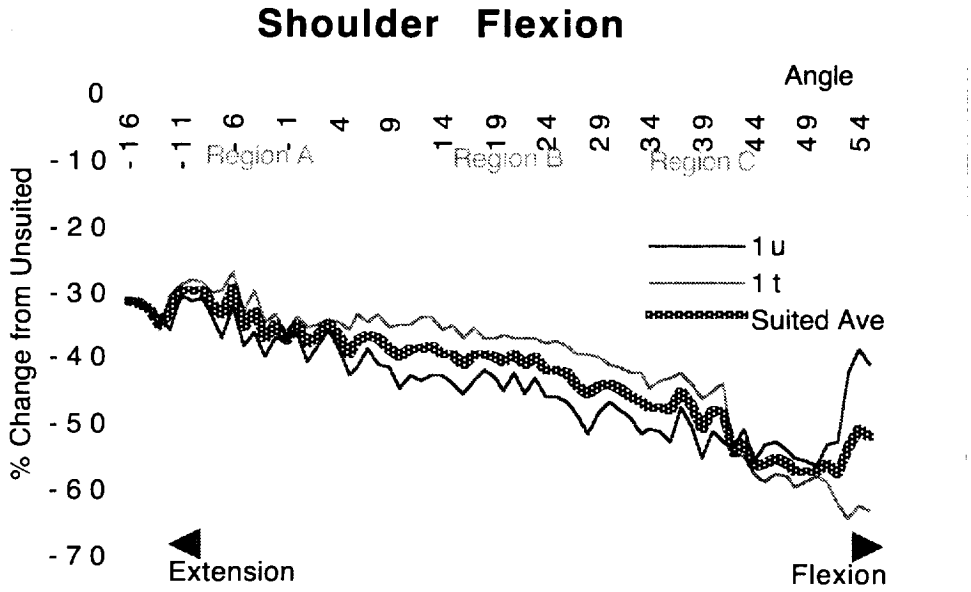

Joint: SHOULDER Flexion
Differences in % Change from Unsuited
****

TOTAL ROM (filtered) <-16 to 55>

	ux	*lu*	*lt*
Ave	-42	1	-1
lt	-40	3	
lu	-43		

REGION A <-16 to 8>

	ux	*lu*	*lt*
Ave	-34	1	-1
lt	-32	3	
lu	-35		

REGION B <8 to 31>

	ux	*lu*	*lt*
Ave	-40	3	-3
lt	-36	7	
lu	-44		

REGION C <31 to 55>

	ux	*lu*	*lt*
Ave	-51	0	0
lt	-52	-1	
lu	-51		

Difference Coefficients, from Unsuited
% Change = B_0 + B_1* angle + B_2* angle^2

	B_0	B_1	B_2
lu:	-38.24	-0.47	0.00
lt:	-31.74	-0.07	-0.01
Ave:	-34.99	-0.27	0.00

Legend:

ux	unsuited
1u	Class 1 suit, no TMG
1t	Class 1 suit with TMG
Ave	Average of both suited conditions

Figure 30 Suited data for shoulder flexion

3.11 External Shoulder Rotation

During external shoulder rotation, *unsuited* torques averaged approximately 15 ft-lb (Fig. 31). Torques tended to decrease from 21 to 12 ft-lb as the angle increased. The trend for suited data was lower (about 10 ft-lb average) and was more constant.

The *suited conditions* each had different trends (Fig. 32). The 1u condition started off much lower (almost 20% lower than condition 1t in Region A) and rose through Regions B and C to surpass both the 1t condition and the unsuited condition. The 1t condition remained relatively constant. Although trends differed, the averages of both conditions were about 29% reduced from the unsuited condition.

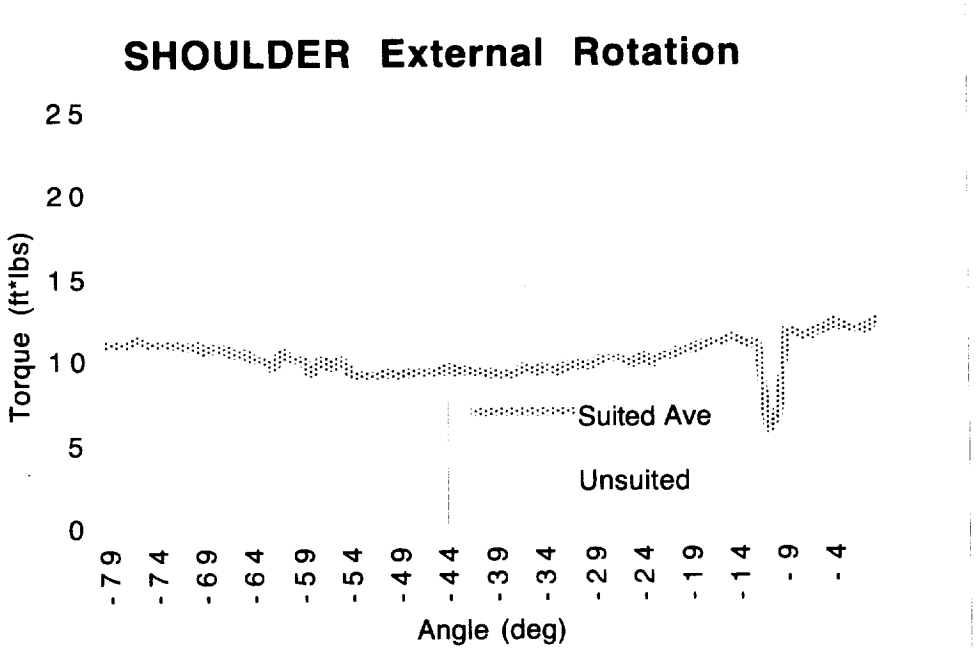

Torque Equation for External Shoulder Rotation
Unsuited Torque = 11.629 – 0.041*angle + 0.001*angle^2

Figure 31 Unsuited data for external shoulder rotation

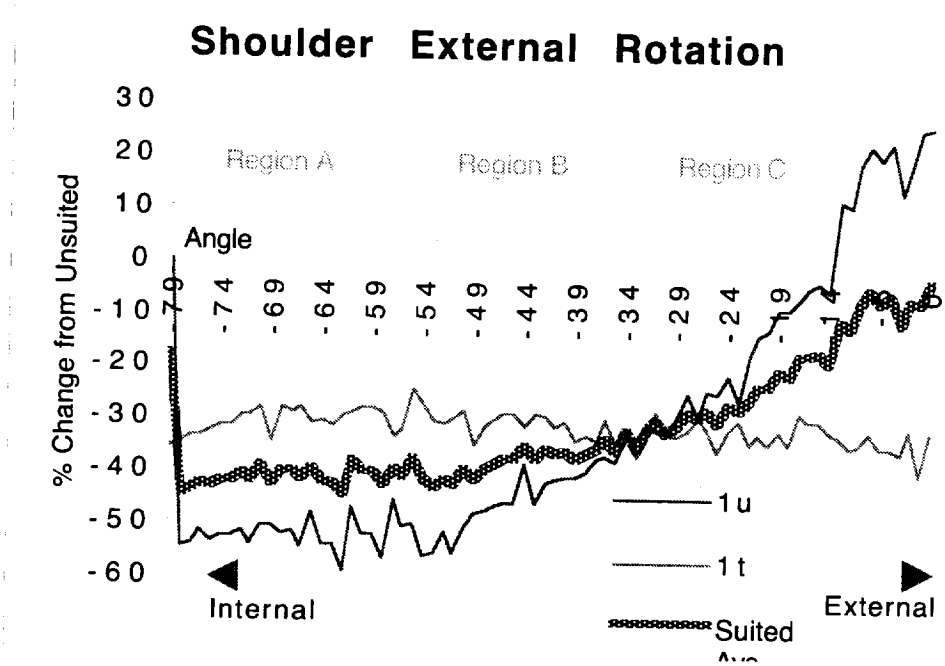

Joint: SHOULDER Rotation, External
Differences in % Change from Unsuited
****

TOTAL ROM (filtered) <-79 to 0>

	ux	*lu*	*lt*
Ave	-29	0	0
lt	-29	-1	
lu	-28		

REGION A <-79 to -53>

	ux	*lu*	*lt*
Ave	-40	9	-9
lt	-30	19	
lu	-50		

REGION B <-53 to -26>

	ux	*lu*	*lt*
Ave	-36	4	-4
lt	-31	9	
lu	-40		

REGION C <-26 to 0>

	ux	lu	lt
Ave	-12	-14	14
lt	-27	-29	
lu	2		

Difference Coefficients, from Unsuited
% Change = B_0 + B_1* angle + B_2* angle^2

	B_0	B_1	B_2
lu:	36.51	2.89	0.02
lt:	-27.63	0.07	0.00
Ave:	4.44	1.48	0.01

Legend:

ux	unsuited
lu	Class 1 suit, no TMG
lt	Class 1 suit with TMG
Ave	Average of both suited conditions

Figure 32 Suited data for external shoulder rotation

3.12 Internal Shoulder Rotation

During internal shoulder rotation, the *unsuited* data showed less variation than the external rotation. The suited average was also higher, averaging 28 ft-lb (Fig. 33). The trend of internal rotation increased slightly at larger angles. The average of all suited conditions displayed this same trend, to a greater extent, but had 26% average lower torques.

Each of the two conditions in the *suited* plots can best be represented as linear difference equations (Fig. 34). Both conditions rose throughout the entire ROM at increasing angles, with the 1u condition (without the TMG) differing less from the unsuited condition. The overall average for the 1t condition was a 34% reduction, and for the 1u condition was an 18% reduction from the baseline.

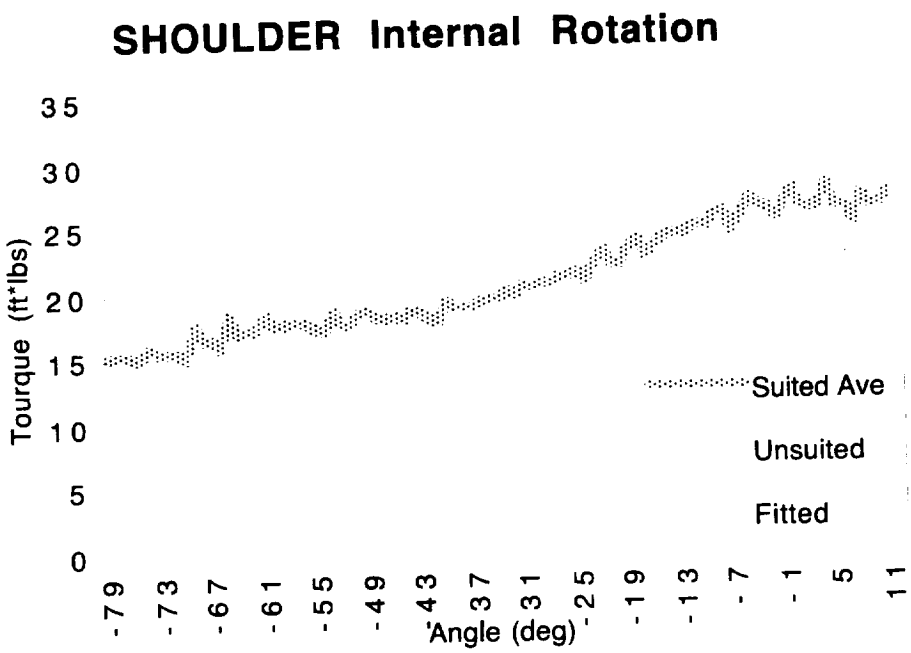

Torque Equation for Internal Shoulder Rotation
Unsuited Torque = 30.261 + 0.126*angle + 0.001*angle^2

Figure 33 Unsuited data for internal shoulder rotation

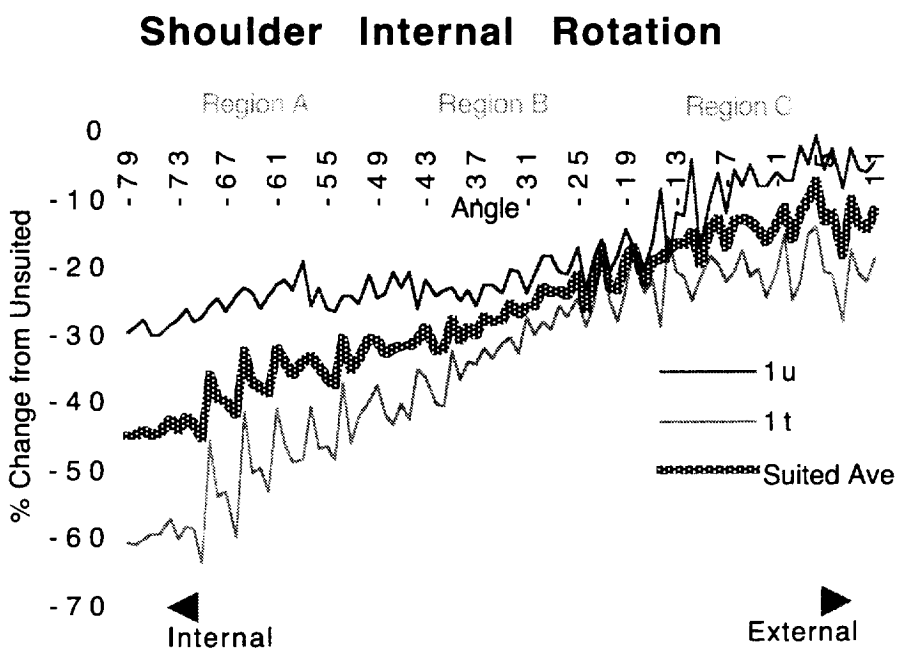

Joint: SHOULDER Rotation, Internal
Differences in % Change from Unsuited
****

TOTAL ROM (filtered) <-79 to 11>

	ux	1u	1t
Ave	-26	-8	8
1t	-34	-16	
1u	-18		

REGION A <-79 to -49>

	ux	1u	1t
Ave	-38	-12	12
1t	-51	-25	
1u	-25		

REGION B <-49 to -19>

	ux	1u	1t
Ave	-27	-5	5
1t	-32	-10	
1u	-21		

REGION C <-19 to 11>

	ux	1u	1t
Ave	-14	-6	6
1t	-20	-12	
1u	-8		

Difference Coefficients, from Unsuited
% Change $=B_0 + B_1$* angle + B_2* angle^2

	B_0	B_1	B_2
1u:	-7.58	0.50	0.00
1t:	-20.11	0.17	0.00
Ave:	-13.85	0.33	0.00

Legend:

ux	unsuited
1u	Class 1 suit, no TMG
1t	Class 1 suit with TMG
Ave	Average of both suited conditions

Figure 34 Suited data for internal shoulder rotation

3.13 Wrist Flexion

Data from the wrist indicated that this joint had the lowest maximal torque when compared to any of the other joint motions examined. In the wrist flexion *unsuited condition*, torques were maximized in the negative end, or extension, of the range (Fig. 35). Starting at 14 ft-lb, these torques fell slightly to about 11 ft-lb at the greatest angle of flexion. The suited wrist condition was higher in magnitude by an average of 10%.

Only two conditions were studied in the wrist *suited* tests, 1t and 3t (Fig. 36). These conditions produced different magnitudes, yet the overall trend of the data was very similar, with the exception of an odd data point at the very end of the ROM. 3t constantly produced torques high above the unsuited torque, averaging 31% above baseline, whereas data for 1t averaged 9% below the baseline.

Region A was flat for both conditions, with 3t averaging 28% and 1t averaging –17%. In Regions B and C, torques from both conditions increased with an increased angle. Region C indicated that 3t averaged 39% and 1t averaged 0% difference from the baseline.

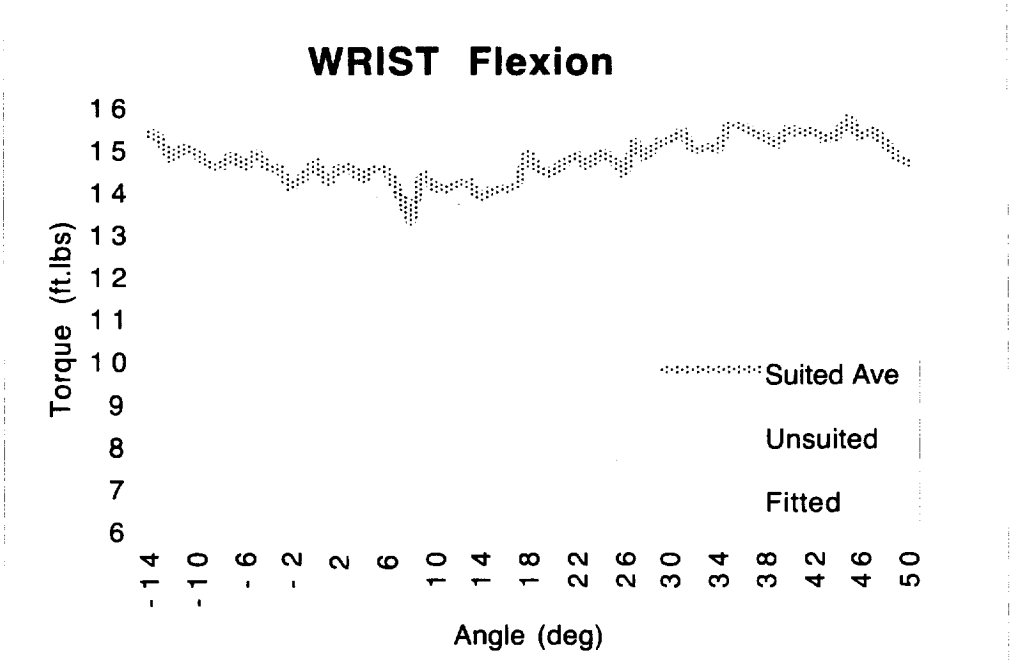

Torque Equation for Wrist Flexion
Unsuited Torque = 13.944 – 0.008*angle – 0.001*angle^2

Figure 35 Unsuited data for wrist flexion

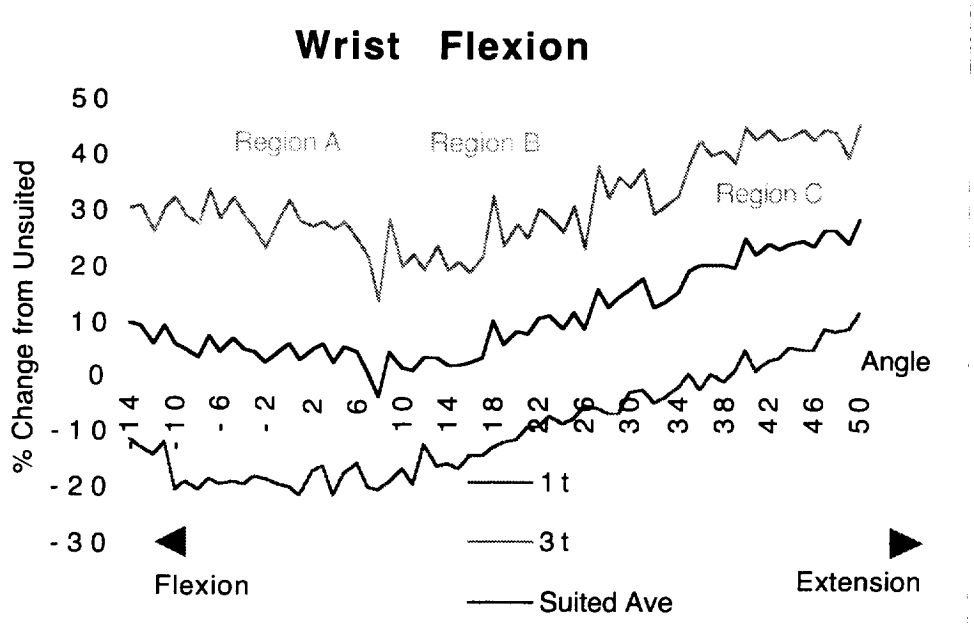

Joint: WRIST Flexion
Differences in % Change from Unsuited
****

TOTAL ROM (filtered) <-14 to 50>

	ux	*1t*	*3t*
Ave	10	20	-20
3t	31	40	
1t	-9		

REGION A <-14 to 7>

	ux	*1t*	*3t*
Ave	5	23	-23
3t	28	46	
1t	-17		

REGION B <7 to 29>

	ux	*1t*	*3t*
Ave	5	18	-18
3t	24	37	
1t	-12		

REGION C <29 to 50>

	ux	*1t*	*3t*
Ave	20	19	-19
3t	39	38	
1t	0		

Difference Coefficients, from Unsuited
% Change = B_0 + B_1* angle + B_2* angle^2

	B_0	B_1	B_2
1t:	-17.74	0.08	0.01
3t:	25.87	-0.23	0.01
Ave:	4.07	-0.08	0.01

Legend:

ux	unsuited
1t	Class 1 suit with TMG
3t	Class 3 suit with TMG
Ave	Average of both suited conditions

Figure 36 Suited data for wrist flexion

3.14 Wrist Extension

The extension movement of the *unsuited* wrist averaged only about 5.5 ft-lb (Fig. 37). With an upward linear slope, the extension peaked at just over 6 ft-lb at the end of motion. The suited average was degraded 13% from the unsuited condition.

Comparison of the two *suited conditions* showed that 1t averaged higher than both the unsuited and 3t conditions (Fig. 38). The 3t condition was 50% below the baseline for much of the motion. The 1t and 3t conditions averaged a difference of 7% and –33%, respectively, from the unsuited condition.

The plots were similar in regional trends. Both conditions started in Region A at about –60% difference from the baseline. The 1t condition had a very steep rise to average –6%, while the 3t condition averaged –52%. Both fell slightly in Region B and rose very steeply again in Region C, converging at the end (most flexed).

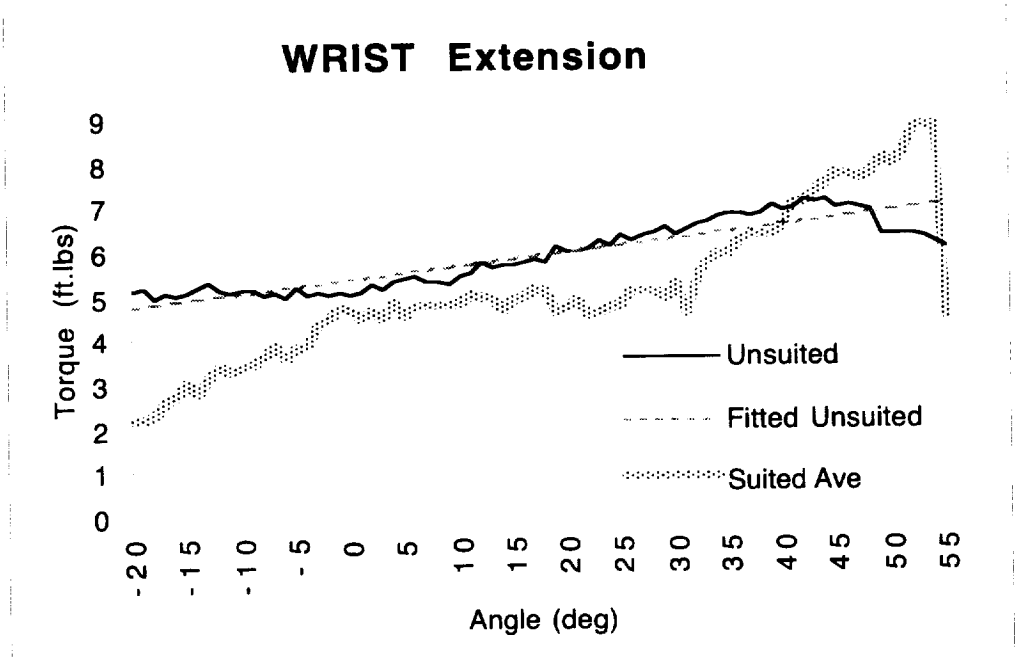

Torque Equation for Wrist Extension
Unsuited Torque = 5.398 + 0.03*angle + 0*angle^2

Figure 37 Unsuited data for wrist extension

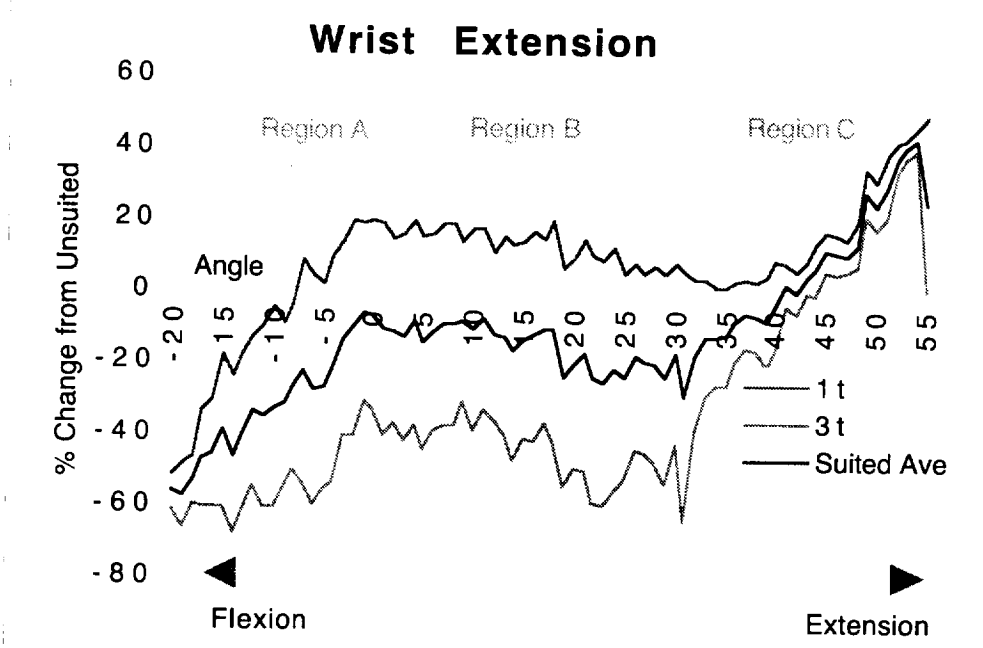

Joint: WRIST Extension
Differences in % Change from Unsuited
****

TOTAL ROM (filtered) <-20 to 55>

	ux	*1t*	*3t*
Ave	-13	-20	20
3t	-33	-41	
1t	7		

REGION A <-20 to 5>

	ux	*1t*	*3t*
Ave	-29	-23	23
3t	-52	-46	
1t	-6		

REGION B <5 to 30>

	ux	*1t*	*3t*
Ave	-16	-28	28
3t	-44	-57	
1t	12		

REGION C <30 to 55>

	ux	*1t*	*3t*
Ave	4	-10	10
3t	-5	-20	
1t	14		

Difference Coefficients, from Unsuited
% Change = B_0 + B_1* angle + B_2*angle^2

	B_0	B_1	B_2
1t:	-0.49	0.91	-0.01
3t:	-54.66	0.22	0.02
Ave:	-27.58	0.56	0.01

Legend:

ux	unsuited
1t	Class 1 suit with TMG
3t	Class 3 suit with TMG
Ave	Average of both suited conditions

Figure 38 Suited data for wrist extension

4. Conclusions

This study's overall goal was to extend the current EMU strength database with a systematic and comprehensive assessment of strength for major joints of the EMU-suited human. Strength data were collected and processed for the isolated joints of six EMU-suited subjects and were compared with their unsuited strength (the numerical results are summarized in Table 6). This report provides the NASA community with a computer-ready database of EMU strength, all regression coefficients, and a library of access routines. It also provides a prediction capability (within the range of data collection) of an individual male's EMU suited strength given his unsuited strength profile. A generic methodology for quantifying the differences between suited and unsuited operations and between different suited conditions has also been established.

Table 6 Summarized Torque Changes for All Motions
Averaged for all suited conditions. Comparison is with respect to unsuited conditions.

Joint Motion	*Region A (% difference)*	*Region B (% difference)*	*Region C (% difference)*	*Total ROM (% difference)*
Elbow Extension	-45	-19	0	-21
Elbow Flexion	-19	-7	-7	-11
Knee Extension	-10	-6	0	-5
Knee Flexion	2	-5	-14	-5
Shoulder Adduction	-40	-28	-13	-27
Shoulder Abduction	-19	-14	-20	-18
Shoulder Extension	-54	-43	-30	-42
Shoulder Flexion	-34	-40	-51	-42
Internal Sh. Rotation	-38	-27	-14	-26
External Sh. Rotation	-40	-36	-12	-29
Wrist Extension	5	5	20	10
Wrist Flexion	-29	-16	4	-13

These data are expected to impact several areas of EMU-related work. For example, designers of new suits will be better able to understand and, therefore, optimize the user's ability to exert force. For instance, the suited elbow in Region A is severely degraded as compared to the unsuited condition (Figs. 16 and 18 and Table 6). In future, suit designers may be able to enhance the performance of the suit in this region. By using the same elbow strength information, human factors engineers and mission planners could better plan tasks that include elbow motions. In instances where elbow extension is the dominant elbow motion, planners should be aware of the extreme decrease in available torque of Region A (Fig. 15). It would be more difficult to maneuver objects in this region; hence, tasks should be planned accordingly. EMU strength model developers could use the prediction coefficients to estimate isolated joint strength.

While current research significantly increases our knowledge of the effect of the Shuttle suit on operator strength, many limitations existed during this experiment that need further evaluation. All strength measurements collected for this report were performed in a seated posture, which is not typically used in EVA. The seated posture was chosen because it allowed data to be collected with minimal modification to the existing hardware. Although a standing posture would have better represented the natural posture of EVA astronauts, isolation of joint strength would be difficult in this position and hardware modifications would have been too costly. The seated posture had the inherent problem that once the suit was pressurized, it had a strong tendency to ride up and away from the subject's shoulder, thus compromising suit fit. In general, however, the seated posture allowed for good restraint and isolation of the joints. Isolation of joints through proper restraints is very difficult when collecting data with suited operators. The wrist was very difficult to secure properly because of the wrist bearing. Inadequacies in the joint restraining system, particularly with wrist flexion and extension, enabled subjects to maneuver themselves without moving the suits' mechanical joints, thus giving them a better physical advantage. This restraint problem resulted

in portions of wrist flexion and extension in the suited condition being greater in magnitude than the unsuited condition, because the subject could slide an elbow forward to assist wrist flexion and pull the elbow back to assist wrist extension. Care must therefore be taken to secure the forearm properly because failure to do so many result in large artificial torque values for the wrist.

In addition to posture, restraint, and isolation issues, ROM was restricted because of hardware on shoulder flexion and extension, shoulder abduction and adduction, and leg flexion and extension strength measurements.

5. Future Direction and Emerging Technologies

This study was a pilot study of six male subjects who all had similar anthropometry. This restriction was imposed owing to suit availability. A more rigorous study, which will include a greater number of subjects and sizes that better represent the astronaut population, will be undertaken. In addition, only select body joints were included in data collection because of hardware limitations. The next study will collect new strength data on three very important motions: ankle dorsi and plantar flexion, hip flexion and extension, and hip abduction and adduction.

Modeling complex systems is becoming feasible with faster hardware and distributed software designers. Planners, engineers, astronauts, and researchers concerned with "person-in-the-loop" activities are relying on computer models of humans and their environments as one of the tools available to assist them in solving space-human factors problems. Results of this and future data collection will be incorporated into a dynamic EMU modeling system. Figure 39 represents the envisioned merging of strength data, kinematics, and a dynamic force model. In these simulations, solutions to questions like "What is the maximum torque that will be imparted at the foot restraint?" or "Which of the joints will most likely get fatigued?" could be better answered.

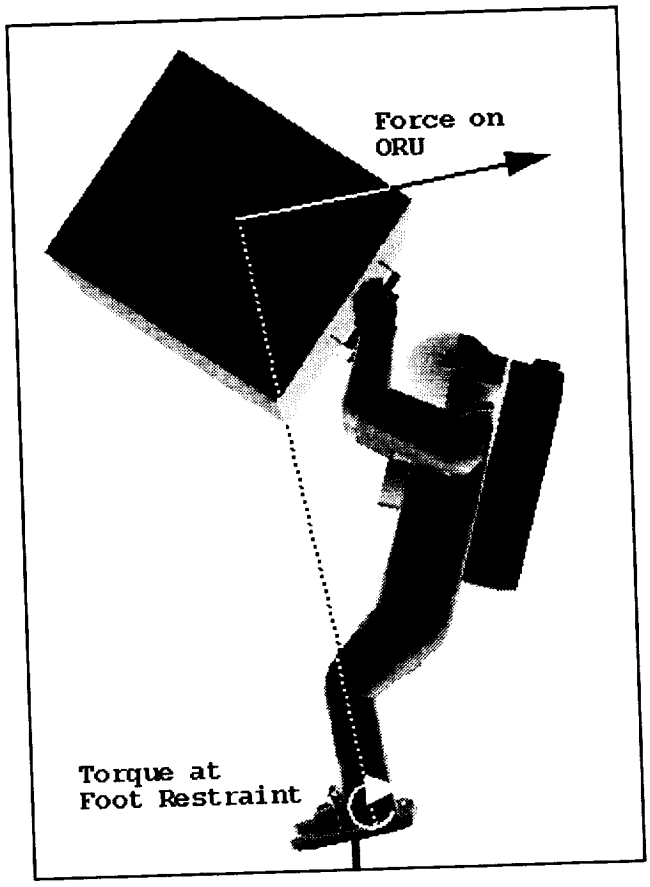

Figure 39 Force and torque evaluation of an EVA

6. Bibliography

Bishu, R. R., and Klute, G. K., "Investigation of the Effects of EVA Gloves on Performance," NASA Technical Paper 3401, October 1993.

Bishu, R. R., and Klute, G. K., "Force Endurance Capabilities for EVA Gloves at Different Pressure Levels," NASA Technical Paper 3420, November 1993.

Bishu, R. R., Klute, G. K., and Byungjoon, K., "Investigation of the Effects of Extravehicular Activity Gloves on Performance," in *Advances in Industrial Ergonomics and Safety V*, edited by R. Nielsen and K. Jorgensen, Taylor & Francis, 1993.

Chaffin, D. B., and Anderson, G. B., *Occupational Biomechanics*, John Wiley & Son, New York, 1984.

Doxey, D., Pandya, A., Aldridge, A., Reschke, M., and Maida, J., "Utilization of a 3D Computer-Human Model for the Analysis of the Change in Postural Control Mechanisms Following Space Flight," Bioengineering Conference, February 1993.

Evans, S., Chaffin, D., and Foulke, J., "A Methodology for Integrating Ergonomic Information in Workspace Design," Proceedings of the Conference on Occupational Ergonomics, 1984.

Gerald, C. F., *Applied Numerical Analysis*, Addison-Wesley Publishing Company, Menlo Park, California, 1970.

Hancock, L. M., Pandya, A. K., and Maida, J. C., "Applications of Capturing Human Motion in a Virtual Reality System," 13th Annual Meeting of the Houston Society for Engineering in Medicine and Biology, University of Houston, Houston, Texas, 1995.

Hasson, S., Pandya, A., Maida, J., Aldridge, A., and Woolford, B., "Use of Lean Body Mass for the Prediction of Isolated Joint and Complex Task Torque," *J Ortho Sports Phys Ther* 15:50, 1992.

Hayes, J. C., McBrine, J. J., Roper, M. L., Harris, B. A., Siconolfi, S. F., and Greenisen, M. C., "Final Report – DSO 477: The Evaluation of Concentric and Eccentric Skeletal Muscle Contractions Following Space Flight," Johnson Space Center, 1992.

Klute, G. K., "Pilot Investigation: Nominal Crewmember Induced Forces in Zero-g," 22nd International Conference on Environmental Systems, SAE Technical Paper Series 921155, Seattle, Washington, July 1992.

LIDO Active Operations Manual, Loredan Biomedical Inc., September 1988.

LIDO Technical Report, Loredan Biomedical Inc., Vol. 1, No. 1, 1987.

Man-System Integration Standards, NASA-STD-3000, Vol. 1, National Aeronautics and Space Administration, 1987.

McKenna, R. F., Pandya, A. K., and Maida, J. C., "Integrating Anthropometry, Strength, and Motion Data into a Human Computer Model," 13th Annual Meeting of the Houston Society for Engineering in Medicine and Biology, University of Houston, Houston, Texas, 1995.

Morgan, D., Pandya, A., and Maida, J., "Towards Modeling of Space Suited Joint Strength," American Society of Biomechanics 19th Annual Meeting, August 1995.

Pandya, A., Hasson, S., Aldridge, A., Maida, J., and Woolford, B., "Correlation and Prediction of Dynamic Human Joint Strength from Lean Body Mass," NASA Technical Report 3207, June 1992.

Pandya, A., Hasson, S., Aldridge, A., Maida, J., and Woolford, B., "The Validation of a Human Force Model to Predict Dynamic Forces Resulting from Multi-Joint Motions," NASA Technical Report 3206, June 1992.

Peters, G., Wilmington, R. P., and Klute, G. K., "Fine Alignment of Large ORUs," JSC Technical Publication JSC-37746, March 1993.

Poliner, J., and Rajulu, S., "Loads Produced by a Suited Operator Performing Took Tasks Without the Use of Foot Restraints," The Proceedings of the 64th Annual Scientific Meeting of the Aerospace Medical Association, Toronto, Canada, May 1993.

Poliner, J., Wilmington, R. P., and Klute, G. K., "Strength Capabilities and Load Requirements While Performing Torquing Tasks in Zero-Gravity," NASA Technical Memorandum in preparation, November 1993.

Rajulu, S., and Klute, G. K., "A Comparison of Hand Grasp Breakaway Strength and Bare-Handed Grip Strength of the Astronauts, SML 3 Test Subjects, and Subjects from the General Population," NASA Technical Paper 3286, January 1993.

Rajulu, S., Fletcher, L., and Klute, G. K., "Evaluation of COSTAR Mass Handling Characteristics in a Frictionless Environment – A Simulation of the Hubble Space Telescope Services Mission," in preparation for publication as a NASA Technical Memorandum, December 1993.

Rothman, W. Erickson, *Statistics: Methods and Application*, Kendall/Hunt Publishing, Iowa, 1987.

Stoycos, L., and Klute, G. K., "An Analysis of the Loads Applied to a Heavy Space Station Rack During Translation and Rotation Tasks," NASA Technical Memorandum 104790, March 1994.

Wilmington, R. P., Poliner, J., and Klute, G. K., "Use of a Pitch Adjustable Foot Restraint System: Operator Strength Capability and Load Requirements," NASA Technical Paper 3477, May 1994.

REPORT DOCUMENTATION PAGE

Form Approved
OMB No. 0704-0188

1. AGENCY USE ONLY (Leave Blank)	2. REPORT DATE	3. REPORT TYPE AND DATES COVERED
	June 1996	NASA Technical Paper

4. TITLE AND SUBTITLE

Comparison of Extravehicular Mobility Unit (EMU) Suited and Unsuited Isolated Joint Strength Measurements

5. FUNDING NUMBERS

6. AUTHOR(S)

David A. Morgan*; Robert P. Wilmington*; Abhilash K. Pandya*; James C. Maida; Kenneth J. Demel

7. PERFORMING ORGANIZATION NAME(S) AND ADDRESS(ES)

Lyndon B. Johnson Space Center
Flight Crew Support Division
Houston, Texas 77058

8. PERFORMING ORGANIZATION REPORT NUMBERS

S-809

9. SPONSORING/MONITORING AGENCY NAME(S) AND ADDRESS(ES)

National Aeronautics and Space Administration
Washington, D. C. 20546-0001

10. SPONSORING/MONITORING AGENCY REPORT NUMBER

TP-3613

11. SUPPLEMENTARY NOTES

*Lockheed-Martin Engineering Science Services, Houston, Texas

12a. DISTRIBUTION/AVAILABILITY STATEMENT

Unclassified/Unlimited
Available from the NASA Center for AeroSpace Information (CASI)
800 Elkridge Landing Road
Linthicum Heights, MD 21090-2934
(301) 621-0390

Subject Category: 54

12b. DISTRIBUTION CODE

13. ABSTRACT *(Maximum 200 words)*

In this study the strength of subjects suited in extravehicular mobility units (EMUs) - or Space Shuttle suits - was compared to the strength of unsuited subjects. The authors devised a systematic and complete data set that characterizes isolated joint torques for all major joints of EMU-suited subjects. Six joint motions were included in the data set. The joint conditions of six subjects were compared to increase our understanding of the strength capabilities of suited subjects. Data were gathered on suited and unsuited subjects. Suited subjects wore Class 3 or Class 1 suits, with and without thermal micrometeoroid garments (TMGs). Suited and unsuited conditions for each joint motion were compared. From this the authors found, for example, that shoulder abduction suited conditions differ from each other and from the unsuited condition. A second-order polynomial regression model was also provided. This model, which allows the prediction of suited strength when given unsuited strength information, relates the torques of unsuited conditions to the torques of all suited conditions. Data obtained will enable computer modeling of EMU strength, conversion from unsuited to suited data, and isolated joint strength comparisons between suited and unsuited conditions at any measured angle. From these data mission planners and human factors engineers may gain a better understanding of crew posture, and mobility and strength capabilities. This study also may help suit designers optimize suit strength, and provide a foundation for EMU strength modeling systems.

14. SUBJECT TERMS

space suits; Shuttle; motion; garments, thermal micrometeoroid; strength; model, computer; extravehicular mobility unit

15. NUMBER OF PAGES
54

16. PRICE CODE

17. SECURITY CLASSIFICATION OF REPORT	18. SECURITY CLASSIFICATION OF THIS PAGE	19. SECURITY CLASSIFICATION OF ABSTRACT	20. LIMITATION OF ABSTRACT
Unclassified	Unclassified	Unclassified	Unlimited